NAVAL POSTGRADUATE SCHOOL
Monterey, California

THESIS

A PRELIMINARY ATTEMPT AT SINTERING
AN ULTRAFINE ALUMINA POWDER
USING MICROWAVES

by

Edgar M. Alhambra

September 1994

Thesis Advisor: I. Dutta/Alan G. Fox

REPORT DOCUMENTATION PAGE

Form Approved OMB No. 0704

1. AGENCY USE ONLY	2. REPORT DATE	3. REPORT TYPE AND DATES COVERED
	22 September 1994	Master's Thesis

4. TITLE AND SUBTITLE: A PRELIMINARY ATTEMPT AT SINTERING AN ULTRAFINE ALUMINA POWDER USING MICROWAVES

5. FUNDING NUMBERS

6. AUTHOR(S) Edgar M. Alhambra

7. PERFORMING ORGANIZATION NAME(S) AND ADDRESS(ES)
Naval Postgraduate School
Monterey, CA 93943-5000

8. PERFORMING ORGANIZATION REPORT NUMBER

9. SPONSORING/MONITORING AGENCY NAME(S) AND ADDRESS(ES)

10. SPONSORING/MONITORING AGENCY REPORT NUMBER

11. SUPPLEMENTARY NOTES The views expressed in this thesis are those of the author and do not reflect the official policy or position of the Department of Defense or the U.S. Government.

12a. DISTRIBUTION/AVAILABILITY STATEMENT
Approved for public release; distribution is unlimited.

12b. DISTRIBUTION CODE
*A

13. ABSTRACT

A commercially available microwave oven was used to sinter ultrafine alumina powders (0.02 -0.05 um particle size) with and without CaO sintering aid. The oven was modified by inserting a thermocouple probe through the bottom housing, and thoroughly insulating the interior with insulating material. The oven was placed in a glove box and filled with argon to prevent degradation of the thermocouple, and oxidation of the powdered graphite susceptor. Heating rates of 50 - 75 Deg C/sec with a maximum temperature of 1575 Deg C were obtained. Limited success in sintering of the the powder compacts was achieved in this preliminary effort. The microstructures of the sintered products were examined by scanning electron microscopy. It was concluded that further work is necessary to develop this technique into one which can be used for the routine sintering of fine powdered ceramic material. A review of the literature on microwave sintering of ceramic powders is also reported.

14. SUBJECT TERMS AUV (1) Sintering, (2) Alumina, (3) Microwaves

15. NUMBER OF PAGES 103

16. PRICE CODE

17. SECURITY CLASSIFICATION OF REPORT	18. SECURITY CLASSIFICATION OF THIS PAGE	19. SECURITY CLASSIFICATION OF ABSTRACT	20. LIMITATION OF ABSTRACT
Unclassified	Unclassified	Unclassified	UL

NSN 7540-01-280-5500

Standard Form 298 (Rev. 2-89)
Prescribed by ANSI STD. 239-18

Approved for public release; distribution is unlimited.

A Preliminary Attempt At Sintering An Ultrafine
Alumina Powder Using Microwaves

by

Edgar M. Alhambra
Lieutenant, United States Navy
B.S., San Jose State University, 1983

Submitted in partial fulfillment
of the requirements for the degree of

MASTER OF SCIENCE IN MECHANICAL ENGINEERING

from the

NAVAL POSTGRADUATE SCHOOL
September 1994

Author: E. M. Alhambra

Edgar M. Alhambra

Approved by: Indranath Dutta

Indranath Dutta, Thesis Advisor

A.G. Fox

Alan G. Fox, Thesis Advisor

Matthew D. Kelleher

Matthew D. Kelleher, Chairman
Department of Mechanical Engineering

ABSTRACT

A commercially available microwave oven was used to sinter ultrafine alumina powders (0.02 -0.05 um particle size) with and without CaO sintering aid. The oven was modified by inserting a thermocouple probe through the bottom housing, and thoroughly insulating the interior with insulating material. The oven was placed in a glove box and filled with argon to prevent degradation of the thermocouple, and oxidation of the powdered graphite susceptor. Heating rates of 50 - 75 Deg C/sec with a maximum temperature of 1575 Deg C were obtained. Limited success in sintering of the powder compacts was achieved in this preliminary effort. The microstructures of the sintered products were examined by scanning electron microscopy. It was concluded that further work is necessary to develop this technique into one which can be used for the routine sintering of fine powdered ceramic material. A review of the literature on microwave sintering of ceramic powders is also reported.

TABLE OF CONTENTS

ACKNOWLEDGEMENT

This work could not have been accomplished without the assistance and support of my fellow students, the dedicated faculty, and especially the staff of the Naval Postgraduate School. Exceptional credit is extended to Dr. Indranath Dutta and Dr. Alan G. Fox for their many hours of patience, guidance, and invaluable assistance in the success of this project. I could not ask for a better collaboration of talent.

A sincere thank you is expressed to my friends and family for their constant encouragement throughout my life. My final and unending appreciation goes to my beautiful and beloved wife, Amelita, for her love, devotion and understanding during the seemingly endless days of study, research, and writing.

I. INTRODUCTION

The word "ceramic" is derived from the Greek word "keramikos" meaning "burnt stuff". The Greeks understood that the necessary material properties of ceramics were conventionally achieved during "firing", a high temperature heat treatment operation utilizing ovens and furnaces known as "kilns" [Ref. C1].

Traditional ceramics, as they are more popularily known, were materials of a clay type mineral composed of a layered structure of hydrated aluminosilicates, like kaolinite [$AL_2(Si_2O_5)(OH)_4$], used in cement constructions, pottery, china-wear, and bricks [Ref. R1]. Other types of ceramics include glasses, refractories, and abrasives (see Fig. 1). However, in recent decades a revolution in materials engineering has ushered in a new generation of ceramics. These advanced ceramics require highly controlled chemical compositions, microstructure, and innovative fabrication techniques. Advanced ceramics now include machined high temperature engine parts, ceramic armor plating, prosthetics, superconducting wire, and electronic packaging [Ref. C1].

Advanced ceramic materials are comprised of oxide ceramics, like alumina (Al_2O_3) and zirconia (ZrO_2), magnetic ceramics like $PbFe_{12}O_{19}$, nuclear fuels like UO_2, and also nitrides, carbides, and borides like Si_3N_4, SiC, and TiB_2.

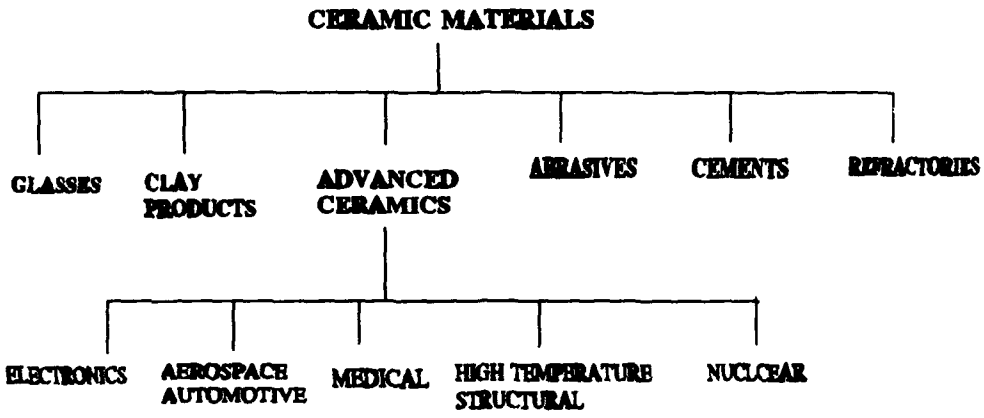

Figure 1: Ceramic materials classification [Ref. C1].

Although a significant portion of the ceramic industry is still devoted to the manufacturing of traditional ceramics, especially cements and glasses, a growing segment has becoming increasingly involved in advanced ceramic structural materials that exhibit a superior combination of high strength at high temperatures, high hardness properties, excellent corrosion and wear resistance, low coefficient of friction and low mass density.

To accompany these advances in material properties, must come advances in material processing, which include methods of heat treatment. Microwave thermal processing could possibly offer a more efficient alternative to conventional heating

with the additional benefit of improved mechanical properties. Microwave heating is a fundamentally different process from conventional radiant element techniques. In conventional heating the surface of the material is first heated by a combination of radiation and convection following which, the interior is heated by thermal conduction, as shown in Figure 2. In microwave heating, power is deposited directly into the material, the ambient air remains relatively cooler than the body, resulting in the development of an inverse temperature profile (see Fig. 3), thus creating a hotter interior than the surface. The characteristics of the profile are dependent upon many factors such as power level, electric field intensity and material properties including lossiness, thermal and electrical conductivity, etc. [Ref. B4]. Understanding the roles played by these factors and thus control over the temperature profile, is the thrust of current microwave research applications.

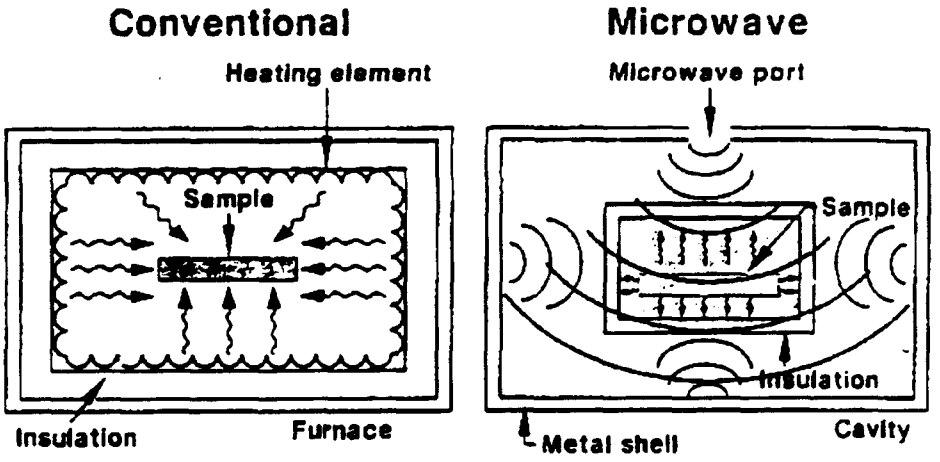

Figure 2: Conventional heating as compared to microwave heating [Ref. S4].

Conventional

External Heating Causes the Centerline Temperature to Lag the Surface Temperature

Microwave

Internal Heating Causes the Centerline Temperature to Lead the Surface Temperature

Figure 3: Temperature profiles for conventional and microwave heating [Ref. J3].

II. CERAMIC POWDER PROCESSING

Most ceramic processing starts with fine powder. Material in a powdered form facilitates the fabrication of complex shapes due in part to its packing properties.

Ceramic powder processing begins with the selection of one or more ceramic powders. Additives, to enhance the fabrication processing or assist the sintering mechanism, may be combined with the powder and then mechanically or chemically processed to achieve proper particle size distribution and proper mixing. The mixture is then formed into its desired shape and finally densified through heat treatment applications.

A. POWDER SELECTION

The selection criteria of raw starting materials is of immense importance for optimizing the final product and must include purity, particle size distribution, reactivity, and polymorphic form as a consideration [Ref. R2].

1. Purity

Purity appreciably affects the advanced mechanical, electrical, optical, or magnetic properties desired. If improved structural properties are sought, purity affects the strength, fracture toughness, and oxidation resistance of the component. Impurities, such as relatively large inclusions,

may act as stress concentrators to diminish a product's tensile strength.

2. Particle Size Distribution

A wide particle size distribution range minimizes the fraction of void space by allowing voids, left by larger particles, to be filled in with smaller particles thus attaining the maximum initial particle packing and uniformity. This will result in minimum shrinkage, low porosity and consistent properties in the final product.

3. Reactivity

Small particles have high surface areas and high free surface energy. The free surface energy is lowered when particles fuse together to form a larger consolidated mass. Thus, lowering the free surface energy is the essential thermodynamic driving force for densification at elevated temperatures. Consequently, the smaller the particle, the greater the potential driving force, and the lower the required sintering temperatures and sintering times. Extended times at elevated temperatures allow grains to grow, diminishing mechanical strength.

4. Polymorphic Form

Many ceramic powders exist in different polymorphic forms, i.e., alpha and beta SiC. One form may be more advantageous for certain processing techniques than another, for example, α-Si_3N_4 versus β-Si_3N_4 in hot pressing [Ref. R1].

B. PROCESSING ADDITIVES

Once the proper selection of powders has been made they are usually combined with liquids, and special additives known as processing aides. These processing aids include binders, lubricants and plasticizers [Ref. R2].

1. Binder

Binders, like polyvinyl alcohol (PVA), and polyvinyl butyral (PVB) are used to provide sufficient strength for handling compacted samples.

2. Lubricant

Lubricants, like zinc stearate and naphthenic acid, are used to decrease interparticle friction as well as tool-die friction during compaction.

3. Plasticizer

Plasticizers, like polyethylene glycol (PEG) and glycerol, promote rheological properties and allow for plastic deformation of the granules. This is especially important for fabricating complicated shapes.

4. Special Additives

Special additives include sintering aides, and grain growth inhibitors. Sintering aids, like CaO and LiF, activate the densification process. Grain growth inhibitors, like MgO in Al_2O_3 processing, limit the size of grain enlargement.

C. POWDER SIZING

The processing of the raw materials to obtain optimum particle size distribution starts with powder sizing. The appropriate powder sizing technique required to prepare the raw materials is fully dependent upon the desired final product. These raw materials can be mechanically or chemically processed. Chemical sizing methods, which minimize contamination and result in better control of the particle size distribution, include precipitation, freeze drying, and sol-gel processing. Mechanical sizing methods, which are simpler and inexpensive, include screening, classifying, elutriation, various milling techniques, etc.

Milling is used when screening, classifying, and elutriation techniques are inadequate to achieve a proper distribution, or a reduction in particle size is required. Ball mills consist of a axially rotating cylinder containing the powder, processing additives, and hardened spheroids or rods as a grinding media. Ball milling can be performed either wet or dry as long as the powder is free flowing. The rate of milling is dependent upon the hardness of the grinding media, and the initial size and specific gravity of the particles. Ball milling produces a broad particle size distribution with an average reduction of particle size to under 5μm [Ref. R2].

D. PRECONSOLIDATION

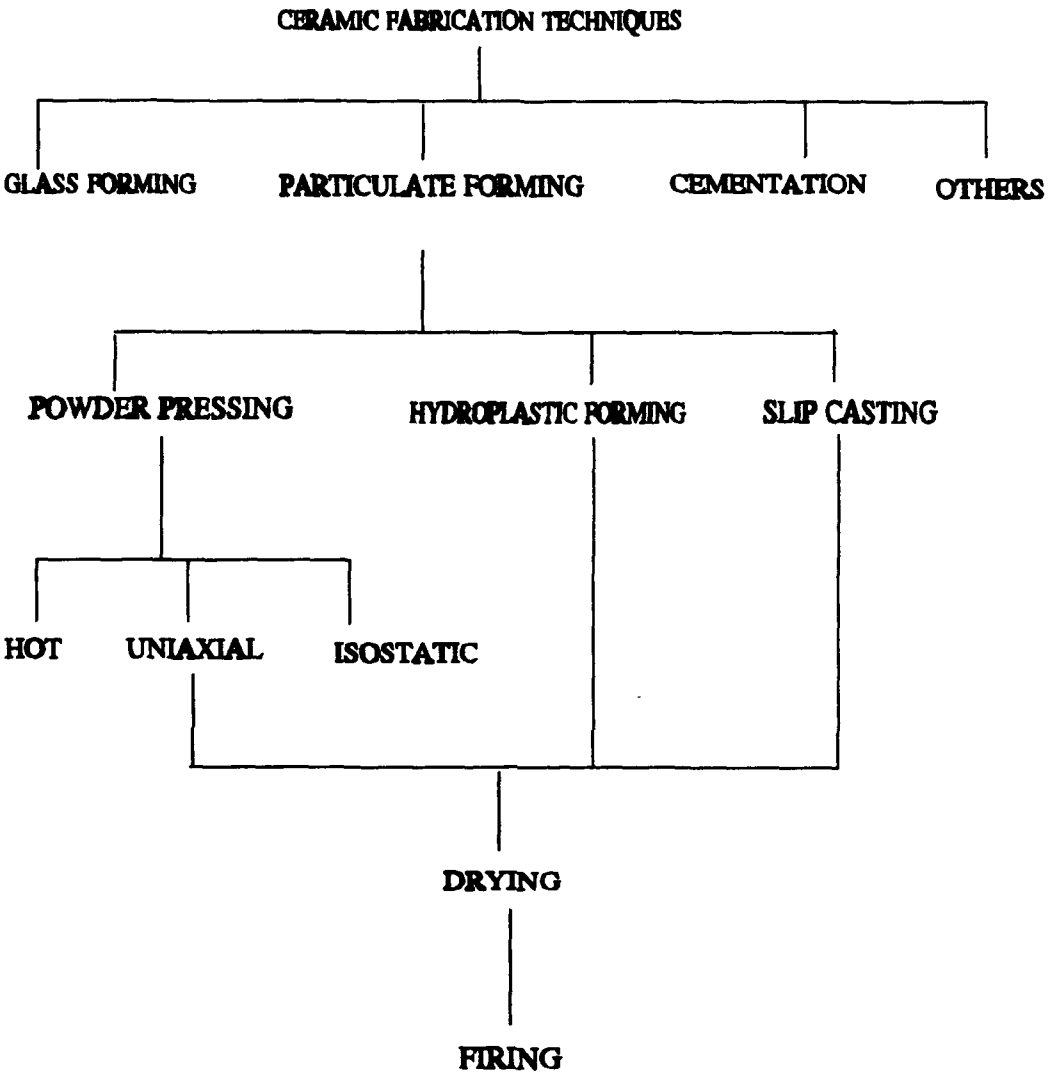

Figure 4: Ceramic fabrication techniques [Ref. C1].

Once the powder has been properly selected, sized, and processed, it is ready for pressing or preconsolidation. The processed powders are dried to remove most of the residual processing liquids. The powders are then formulated into their desired shape by either powder pressing, hydroplastic

forming, or slip casting (see Fig. 4). In the pressing technique, the dried powder is pressed in a punch and die assembly to produce an unfired compact material known as a green body.

There are three methods of powder pressing; uniaxial, isostatic, and a modified process that combines preconsolidation and heat treatment known as hot pressing [Ref. C1].

1. Uniaxial Pressing

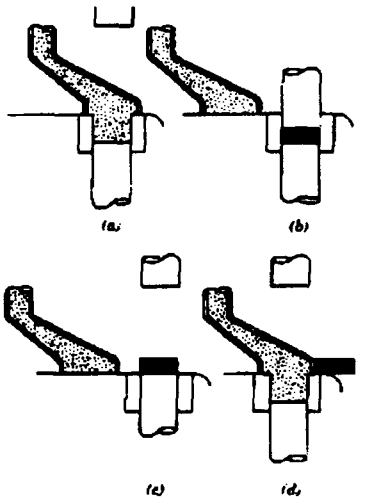

Figure 5: Uniaxial pressure technique in industry [Ref. C1].

Uniaxial pressing is restricted to simple shapes but can be rapidly and inexpensively reproduced. Here, the processed powder is compacted in a punch and die assembly by a single force in the axial direction. Figures 5 and 6 show

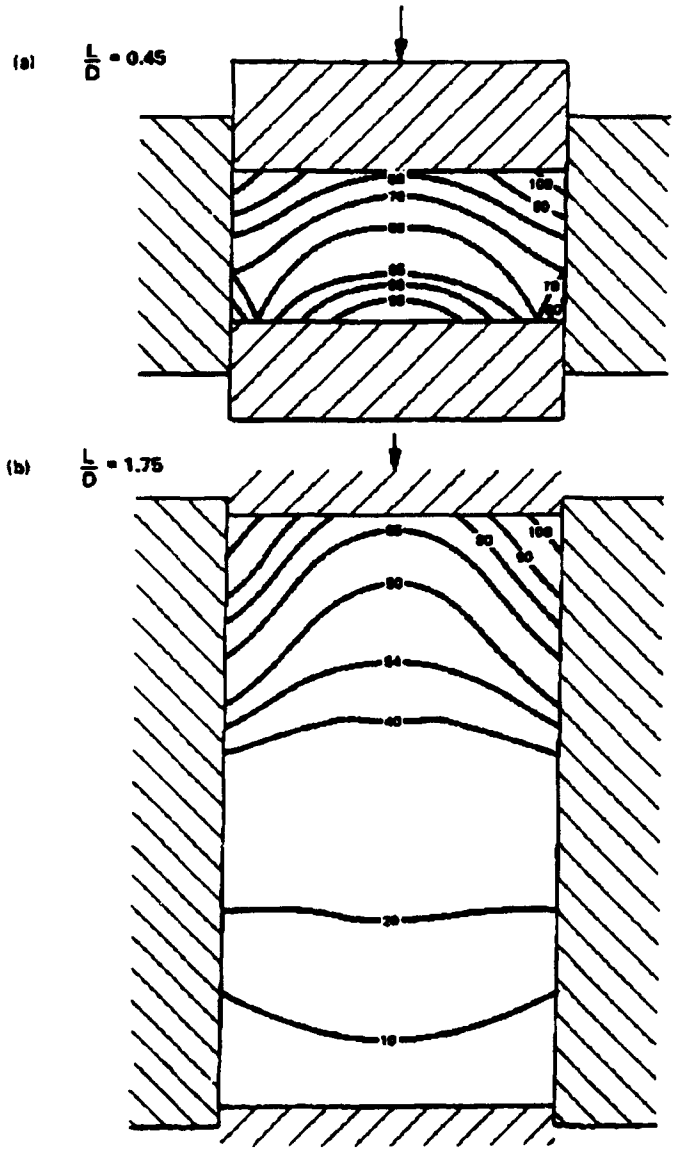

Figure 6: Pressure variations in uniaxial pressing [Ref. C1].

a uniaxial pressure technique applied in high speed production and the resulting pressure variations due to inter-particle and tool-die friction in both small and large sample sizes. A more uniform packing result from smaller sized samples.

2. Isostatic Pressing

In isostatic pressing much more complicated shapes are possible but production rate is slow. In this case, the processed powder is contained in a liquid tight rubber mold, then placed in a thick walled steel pressure vessel. Hydrostatic pressure is utilized to distribute force equally in all directions.

3. Hot Pressing

Under hot pressing, powder compaction and heating are conducted together at elevated temperatures. This is an expensive and time consumming method of fabrication, but high densities with limited grain growth can be achieved. It is a practical procedure for materials that require extremely high temperatures before forming a liquid phase.

E. HEAT TREATMENT

The green product undergoes consolidation in three stages of heat treatments; binder burn-out, sintering, and cool down, before arriving at the final sintered product [Ref. R1].

1. Binder Burn-out

This is the first stage during which binder is eliminated along with decomposition gases. Binders may be an organic or inorganic additive. If it is inorganic it remains in the final product. A binder material which is an organic compound will leave a carbon residue and if not completely

burned-off may cause undesirable localized chemical reactions or crack formations in the sintered product.

2. Sintering

Table I: SINTERING CLASSIFICATIONS AND TRANSPORT MECHANISMS [Ref. C1].

Type of sintering	Material transport mechanism	Driving energy
Vapor phase	Evaporation-condensation	Differences in vapor pressure
Solid state	Diffusion	Differences in free energy or chemical potential
Liquid phase	Viscous flow, diffusion	Capillary pressure, surface tension
Reactive liquid	Viscous flow, solution-precipitation	Capillary pressure, surface tension

In the sintering stage, there is a reduction in porosity accompanied by a shrinkage in dimensions contributing to an improvement in material integrity. The removal of porosity in the green product involves a chemical bonding between adjacent particles and a subsequent increase in density and material strength. Sintering is divided into four classifications, but each requires a mechanism for mass

transport and energy to initiate and sustain the transport mechanism (see Table I) [Ref. R1].

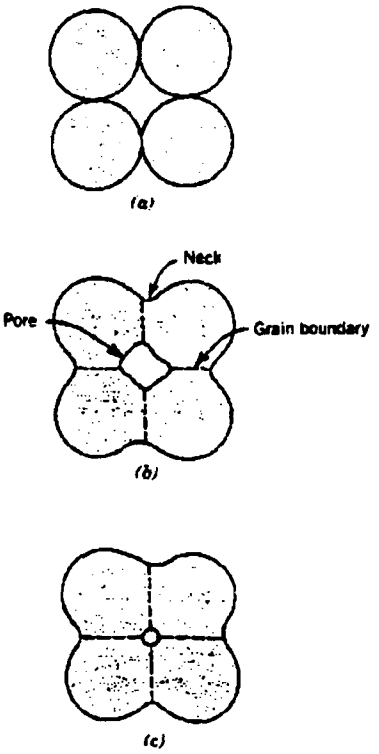

Figure 7: Powder sintering steps. (a) Powder after compaction. (b) Sintering begins and poreforms. (c) Sintering continues with a corresponding decrease in pore size [Ref. C1].

Solid-state sintering is conducted below the melting temperature of the material, and a liquid-phase is not normally present [Ref. C1]. The mechanism of material transport is diffusion, and the thermodynamic driving force is the difference in free-energy between the free surfaces of the particles and the bonding regions between adjacent particles. Figure 7 shows the steps in solid state sintering. By the addition of CaO as a sintering aid, some liguid phase

sintering occurs between adjacent particles which facilitates the sintering process.

3. Cooling

The last step in the heat treatment process is cooling of the densified product. Cooling rates must be carefully controlled to reduce stress cracks resulting from severe thermal gradients between the hot interior and the relatively cooler surface. After cooling the product is finally ready for machining and quality inspection.

III. MICROWAVE PROCESSING

A. WHY MICROWAVE PROCESSING?

Initially, microwave heating served as a more efficient method of converting electrical energy to thermal energy as compared to conventional heating. Other important benefits, like uniform volumetric heat distribution, and extremely high and rapid temperature rate increases, are directly associated with the rapid conversion of electromagnetic energy to thermal energy that is characteristic of microwave heating. Microwave sintering offers advantages over conventional methods that fall primarily into two categories, improved mechanical properties and increased efficiency.

1. Improved Mechanical Properties

The prospect of improved mechanical properties through microwave sintering is based on a rapid uniform volumetric heating process [Refs. M2 and B4]. This is expected to minimize residual thermal stresses and crack formation during sintering thus allowing for fabrications of larger samples with more complicated shapes. Conventional radiant element heat treatment techniques rely on energy heating the surface of the ceramic component by a combination of radiation and convection, from there it is thermally conducted towards the cooler interior of the component. Since most ceramic

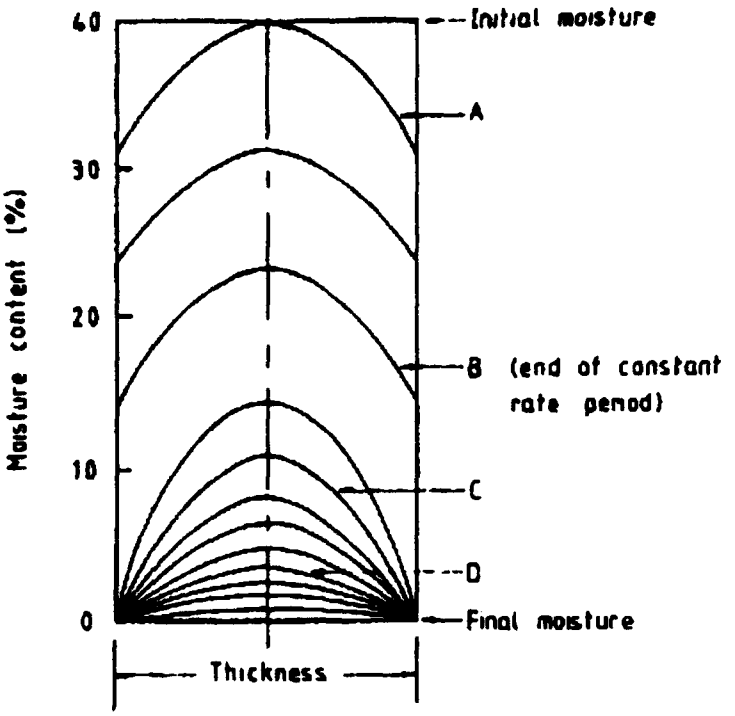

Figure 8: Conventional drying profile [Ref. B1].

materials are excellent thermal insulators, the rate at which heat energy penetrates a large mass can be very slow, leading to severe temperature gradients. Temperature gradients will continue to exist until thermal equilibrium is achieved between adjacent parts [Ref. K1]. As a consequence of thermal expansion and the brittle nature of ceramics, this can result in the surface expanding more than the center, leading eventually to crack formation. Heating rates using conventional methods are therefore severly limited, to less than 5-10 Deg C/min [Ref. B2]. Control of the temperature profile during microwave sintering to improve temperature uniformity across the entire ceramic (see Figs. 8 and 9) can

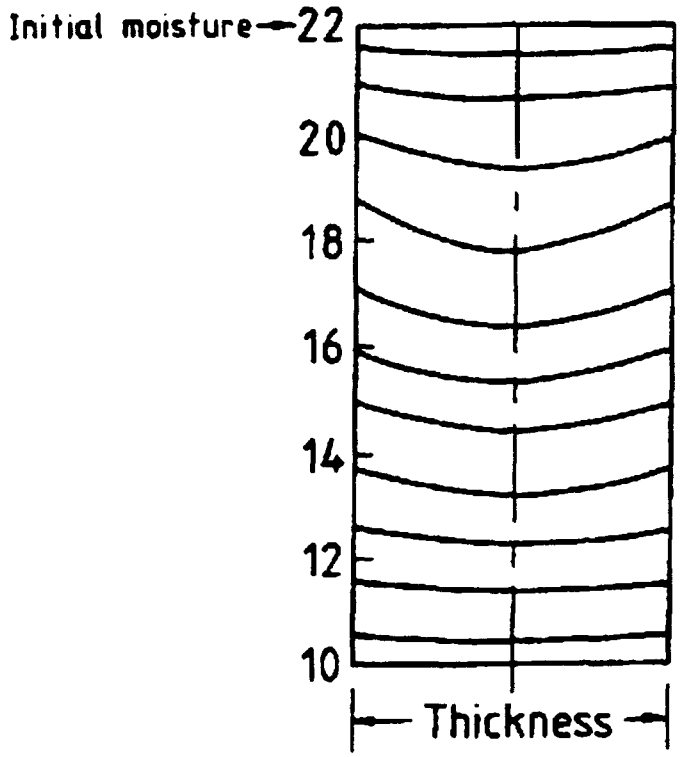

Figure 9: Microwave drying profile [Ref. B1].

allow much higher heating rates with diminished differential expansion [Ref. M2]. Cooling can present similar problems to heating. In this case, the surface of the material contracts faster than the interior and the component undergoes tensile stresses. Since ceramic materials are weak in tension, this often restricts cooling rates to as little as 3-5 Deg C/min to avoid thermal stresses [Ref. B2]. However, again by controlling the temperature profile during the cooling stage, a slightly faster cooling rate is acceptable.

Another potential advantage, obtainable with microwave heating, is the possibility of sintering ceramics from the inside out [Refs. B3 and B4]. Consider two cases, a

processing condition where the sintering of a ceramic body requires maintaining a particular atmosphere in contact with every powder particle, or the removal of entrapped gas. With conventional sintering the first region to densify is the surface of the component where the temperature is hottest. The result is the closing of surface passages needed to allow the desired atmosphere to remain in contact with the interior portion or preventing entrapped undesirable gases to escape. Inferior properties would result since the solution selected either involves deliberately leaving open porosity through the body or allowing entrapped gases to remain and cluster into pockets. Both severely reduce mechanical strength and integrity. By controlling the inverse temperature profile it may be possible to cause the ceramic to sinter from the inside out, thus eliminating the need to terminate the sintering process while open porosity still exists, or in the case of entrapped gas, leaving pockets of gas enclosed in the product.

Since the absorption of microwave energy appears to vary with the composition and structure of different phases, selective heating is possible creating structures with useful and unusual properties [Ref. B4]. Dielectric properties of individual ceramic phases differ depending on parameters such as composition, microstructure, etc. A ceramic containing multiple phases is expected to behave in a non-homogeneous manner in a microwave field. For example, silicon carbide particles will heat faster than an alumina matrix [Ref. W1].

A theory that applies to all rapid sintering techniques predicts that microwave sintering of ceramics and composites, with the associated reduction in processing time and temperature will result in higher sintering rates, higher diffusion rates, and finer grained microstructure. Microwave processing can also lead to a uniform temperature distribution resulting in uniform shrinkage during sintering and thus a more uniform microstructure [Ref. K1].

2. Increased Efficiency

The assumption of higher efficiency is also based on the rapid volumetric heating effect of microwaves. Since microwaves penetrate the dielectric with absorption and heat generation throughout the material, the heating process is much more efficient, possibly as high as 80-90%. Direct volumetric heating of the work piece is expected to result in less expensive heating due to the anticipated use of less energy, less insulation, and the absence of furnace parts such as heating elements and extensive structural housing. Additionally anticipated savings arise from the speed of microwave heating, which can be a hundred times faster than conventional heating. While cool down times remain the same, substantial energy savings would result from the extremely rapid heat-up rates. Rapid heat-up rates would lead to significantly lower processing times and larger output rates and consequently more efficient usage of capital equipment.

Cost accounting estimates concerning the benefits of microwave applications predict annual operating cost reductions of 20-30%, with energy usage reductions of greater than 50% [Ref. C2]. Other benefits include higher throughput rates, higher quality, and higher product reliability [Ref. C2]. Table II

Table II: ADVANTAGES OF MICROWAVE PROCESSING OVER CONVENTIONAL METHODS [Ref. S4].

Direct coupling (absorbing) of microwave creates volumetric (bulk) heating	• Potential to heat large sections uniformly • Reversed thermal gradients: surface cooler than interior • Process materials at lower surface temperatures • Rapid removal of water, binders, and gases without rupture or cracking • Internal stresses reduction by lower thermal gradients • Heat in clean (pure) environment: air, controlled atmospheres, vacuum, or pressure • Control partial pressure of reactive gases for selective oxidation/reduction of certain phases • Improvement of product quality, uniformity, and yields • Instantaneous response to microwave power changes • Low thermal mass; precise and automated temperature control
Dielectric losses (and heating) accelerate very rapidly with increasing temperatures above T_m	• Ability to heat "transparent" materials above T_m • Very rapid processing (2 to 50 times faster than conventional) • Densify materials rapidly with minimum grain growth (accelerated sintering) • Reduce process costs (time, energy, and labor) • Ability to heat ceramics well above 2000°C (in air, vacuum, or controlled atmospheres)
Microwaves are polarized and coherent; location of maximum electric and magnetic fields can be controlled	• Capability of high-energy concentration in short times and in selected regions • Frequency and power level optimization for given material, size, and shape • Potential for process automation, flexibility, efficiency, and energy savings • Precise heating of selected regions, ie., brazing or sealing of joints, fiber drawing, and plasma generation • Acceleration of sintering and diffusion due to high electrical fields; thus densification at lower temperatures
Differential microwave coupling of phases, additives, and constituents leads to selective heating	• Synthesis of new materials and microstructures • Heating of selected zones (brazing and sealing) • Enhanced coupling of microwave transparent materials • Use of fugitive coupling materials for preheating of otherwise transparent materials • Use of microwave-coupling materials as shapes or containers to heat the more transparent materials • Superior control over state of oxidation through selective heating of phases and control over oxygen partial pressure

summarizes some of the advantages of microwave processing over conventional methods.

Thus, the primary reason for the growth in using microwaves to process ceramic materials as opposed to conventional ovens are the rapid internal, uniform, and volumetric heat generation leading to improved material

quality and mechanical properties, and the reduction in cost, time, and energy.

B. MICROWAVE RADIATION

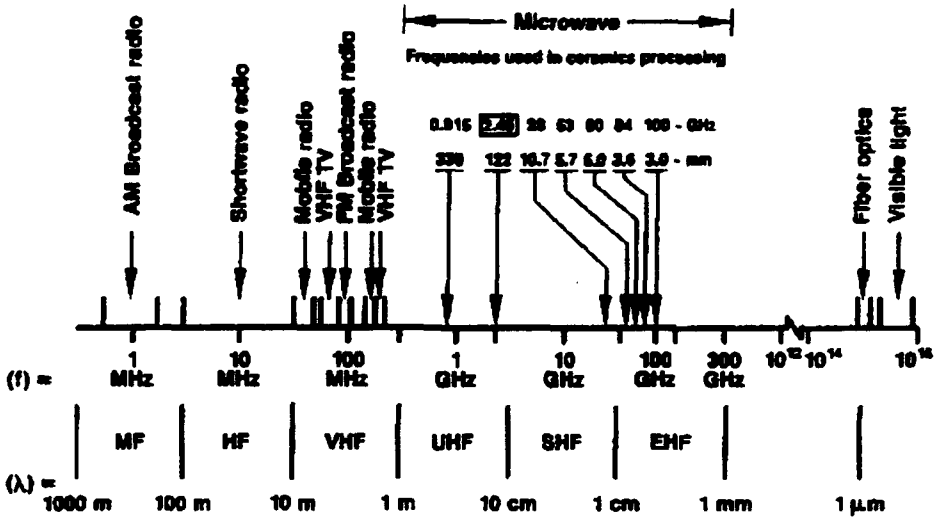

Figure 10: The electromagnetic spectrum showing the microwave band [Ref. S2].

A discussion of microwave radiation must begin with the electromagnetic spectrum. The range of microwave energy is the portion from 300 MHz to 300 GHz with corresponding wavelengths of 1 m to 1 mm [Ref. B5]. This range falls between radiowaves and visible light on the electromagnetic spectrum (see Fig. 10). To prevent interference with telecommunications, defense, and maritime operations, several distinct bands have been allocated for, Industrial, Scientific and Medical (ISM) purposes, the frequency range utilized for microwave heating falls between 400 MHz to 40 GHz (see Table

Table III: MICROWAVE FREWUENCIES ALLOCATED FOR ISM USAGE [Ref. B1].

Frequency MHz	Frequency tolerance ±	Area permitted
433.92	0.2%	Austria, Netherlands, Portugal, Switzerland, West Germany, Yugoslavia.
896	10 MHz	Great Britain.
915	13 MHz	North and South America.
2375	50 MHz	Albania, Bulgaria, Czechoslovakia, Hungary, Rumania, USSR.
2450	50 MHz	Worldwide except where 2375 MHz is used.
3390	0.6%	Netherlands.
5800	75 MHz	Worldwide.
6780	0.6%	Netherlands.
24150	125 MHz	Worldwide.
40680		Great Britain.

III). The principal frequencies used, where manufactured equipment is easily available are 433 MHz, 915 MHz, and 2.45 GHz [Ref. B1]. Microwaves behave similarly to other forms of electromagnetic radiation and possess the characteristics of any electromagnetic propagation, for example, wavelength, frequency, magnitude, straight line propagation, and point to point energy transfer. Like radiowaves, they are generated at a source, transmitted, absorbed by some materials and reflected by others.

1. Microwave Generation

Microwaves can be generated from electron tubes, magnetrons, klystrons or gyrotrons. Klystrons and gyrotrons have greater power and efficiency, but require an extensive external means of cooling. For most industrial purposes, and domestic applications, the continuous wave magnetron is employed because of its simple construction, low production cost, and reliability [Ref. P2].

2. Microwave Transmission

Below 500 MHz radio frequency signals can be transmitted through conventional wires. At microwave frequencies, above 500 MHz, wired circuits cannot efficiently transfer power. Waveguides serve as a conduit to transfer power from the source to the applicator, the cavity containing the material to be heated [Ref. Y1]. Microwaves propagate through the waveguide in a zig-zag fashion, repeatedly being reflected off the surrounding walls. Waveguides are usually constructed with high conductivity copper to minimize power transmission losses. Waveguide dimensions depend on the operating frequency and are carefully designed to eliminate arcing and minimize power reflections back to the source and generally have rectangular or circular cross-sections [Ref. K1].

3. Microwave Absorption and Reflection

With the development of radar transmission, it was discovered that some materials reflect electromagnetic radiation while others absorb them. A discussion of microwave absorption and reflection properties must begin with the fundamentals of the interaction of electromagnetic fields with dielectrics.

C. MICROWAVE-DIELECTRIC INTERACTION

Certain materials, i.e., insulators, increase in temperature when subjected to high frequency electromagnetic waves. This increase in temperature is caused by a transfer of energy from the microwave frequency radiation to the dielectric by primarily two physical mechanisms; polarization and conductive currents.

1. Polarization

When insulating materials are subjected to an electric field, the electric field induces polarization of charged particles due to the relative displacement of positive and negative charges at the molecular or atomic level. Dielectric heating is a result of the electric field's ability to polarize the charges in a material, and with increasing frequency, the inability of the polarization to remain in step with the rapid oscillations of the sinusoidal electric field. The resulting polarization field vector **P** lags the externally applied electric field, **E**. The resulting current density **J**,

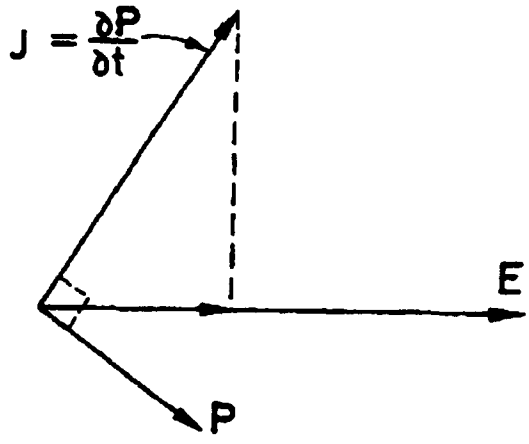

Figure 11: Diagram showing phase relationships between the electric field, polarization, and current density [Ref. B1].

which equals d**P**/dt, retains a component in phase with the applied electric field (see Fig. 11). Power, which equals **E**dP/dt, is now extracted continuously from the electric field and is dissipated as heat in the dielectric [Ref. B4].

The incident electromagnetic field produces electronic, ionic, interfacial, and reorientation polarization (see Fig. 12).

a. Electronic Polarization

Electronic polarization is due to the shift of the valence electron cloud relative to the nucleus. This polarization mechanism occurs at very high frequencies (10^{15} Hz) in the ultraviolet and optical range.

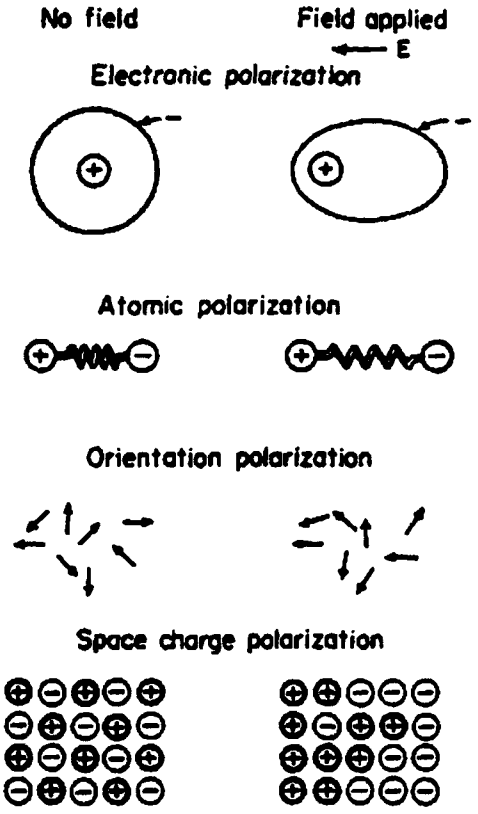

Figure 12: Mechanisms of polarization [Ref. V1].

b. Ionic Polarization

Ionic polarization or atomic polarization, is the displacement of positive and negative ions in the material with respect to each other. This mechanism occurs in the infrared frequency range (10^{12} - 10^{13} Hz).

c. Interfacial Polarization

Interfacial, space-charge, or Maxwell-Wagner polarization occurs in heterogeneous dielectrics when one component has a higher conductivity than the other. It is related to the charge buildup in the interfaces between components in heterogeneous systems. It is usually associated with the presence of impurities forming a separate and somewhat conducting phase. The frequency range for interfacial polarization, though usually quite low 10^{-3} Hz may extend to fairly high frequencies in the kilocycle range 10^{3} Hz.

d. Orientation Polarization

This type of polarization, involves the perturbation of the thermal vibration of ionic or molecular dipoles, producing a net dipolar orientation in the direction of the applied field. Orientation polarization mechanisms can be divided into two categories. In the first case, molecules containing a permanent dipole moment may be rotated against an elastic restoring force about an equilibrium position. The second mechanism of orientation polarization is an especially important contribution to the room temperature dielectric behavior of glasses and ceramics. This type of polarization occurs largely as a result of the motion of charged ions between the interstitial positions within the ionic structure of the material.

Electronic, ionic, and interfacial polarization occur primarily outside the microwave frequency range. The most significant polarization in the microwave frequency range is orientation polarization and occurs in the frequency range of 1-10 GHz [Ref. B4]. Orientation polarization is usually the dominant mode of energy absorption.

2. Conductive Currents

Among all the possible forms of loss mechanisms, orientation polarization is probably the most significant in industrial microwave heating applications at frequencies above 1 GHz. There is another type of energy absorption mechanism that occurs in the radio frequency range and extends to the lower end of the microwave frequency range (1-1000MHz). Here, the applied electromagnetic field induces conductive current flow resulting in a resistance heating related to an ohmic type of energy loss [Ref. B4]. This loss is proportional to the electrical conductivity of the material.

D. MATHEMATICAL CONCEPTS

A mathematical development of the microwave-dielectric interaction would be too extensive to cover here. Various authors including Von Hippel [Ref. V1] and Metaxes [Ref. M7] provide thorough coverage of the subject. Only those mathematical concepts that are frequently encountered in the reviewed literature will be briefly discussed.

1. Total Effective Dielectric Loss

The two primary physical energy absorbing or, loss mechanisms, thru which energy can be transferred to a ceramic material are orientation polarization and conductive flow losses.

Mathematically both can be combined in the total effective dielectric loss factor [Refs. M6 and S1],

$$\varepsilon''_{eff} = \varepsilon'' + \sigma_d/\omega\varepsilon_o \qquad (1)$$

where,

ε''_{eff} = total effective dielectric losses

ε'' = orientation losses

$\sigma_d/\omega\varepsilon_o$ = conductivity losses

σ_d = dielectric conductivity

ω = frequency

ε_o = permittivity of free space

Both polarization and conductive current flow deposit power volumetrically into the dielectric sufficiently to raise the temperature required for sintering, 1400-2000 Deg C, provided that heat losses from the material are restricted [Ref. B4].

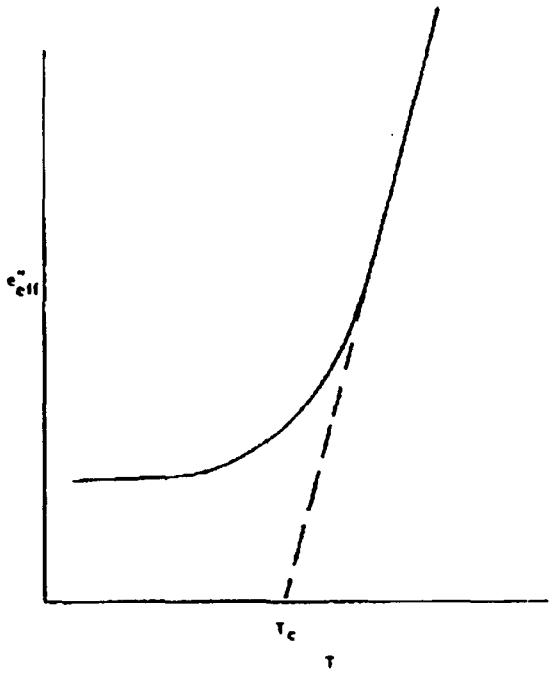

Figure 13: Qualitative representation of loss factor [Ref. M7].

The total effective dielectric loss factor determines how readily a ceramic couples with the incident microwave field. At a total loss of less than 0.01 and the ceramic is considered a low-loss dielectric. If the total loss ranges between 0.05 and 1.0, the ceramic material should encounter no coupling difficulties. Materials with very large loss factors, so readily absorb microwave energy that the depth of penetration of the radiation is very small so that only the surface of the sample is heated, resembling conventional heating [Ref. M6]. Table IV shows the dielectric properties of various ceramics. Figure 13 shows a qualitative

Table IV: DIELECTRIC PROPERTIES OF SOME CERAMICS [Ref. B1].

Material	ρ	T	ρ	E-field direction	frequency 10^9 Hz		frequency 3×10^9 Hz	
	gcm^{-3}	°C	ohmcm		ϵ'	ϵ''_e	ϵ'	ϵ''_e
Silicon carbide		25	35		107	73.4	60	34.8
BeO + SiC				∥	23-75	2.3-30	20-60	3-27
Zinc oxide		25	100	⊥	11	17	8.5	10
Alumina (Al-500)	3.665	25			9	0.056	9	0.063
Alumina (Al-18)	3.676 3.675	25 500			9.1 9.7	0.0025 0.02		
Zirconia		25			3	0.04		
Boron nitride		25 25		⊥ ∥	3.5 4.9	3×10^{-4} 1×10^{-3}		
Steatite		25			6.9	3.5×10^{-4}	6.9	3.5×10^{-4}
Magnesia		500			7.1	1×10^{-3}	7.08	7.5×10^{-4}

representation, for most ceramic materials, of how loss factor varies as a function of temperature, and the critical temperature, T on the diagram, is where the material readily couples with the microwave radiation.

An alternative, and more often used expression for losses is the effective loss tangent which is the ratio of the total effective loss factor over the relative dielectric constant.

2. Loss Tangent

A measure of the absorption capability of microwaves by a material is the effective loss tangent [Ref. S1].

$$Tan\ \delta_{eff} = \frac{\varepsilon''_{eff}}{\varepsilon'} = \frac{\varepsilon''}{\varepsilon'} + \frac{\sigma_d}{\omega\varepsilon'\varepsilon_o} \qquad (2)$$

where,

ε' = relative dielectric constant

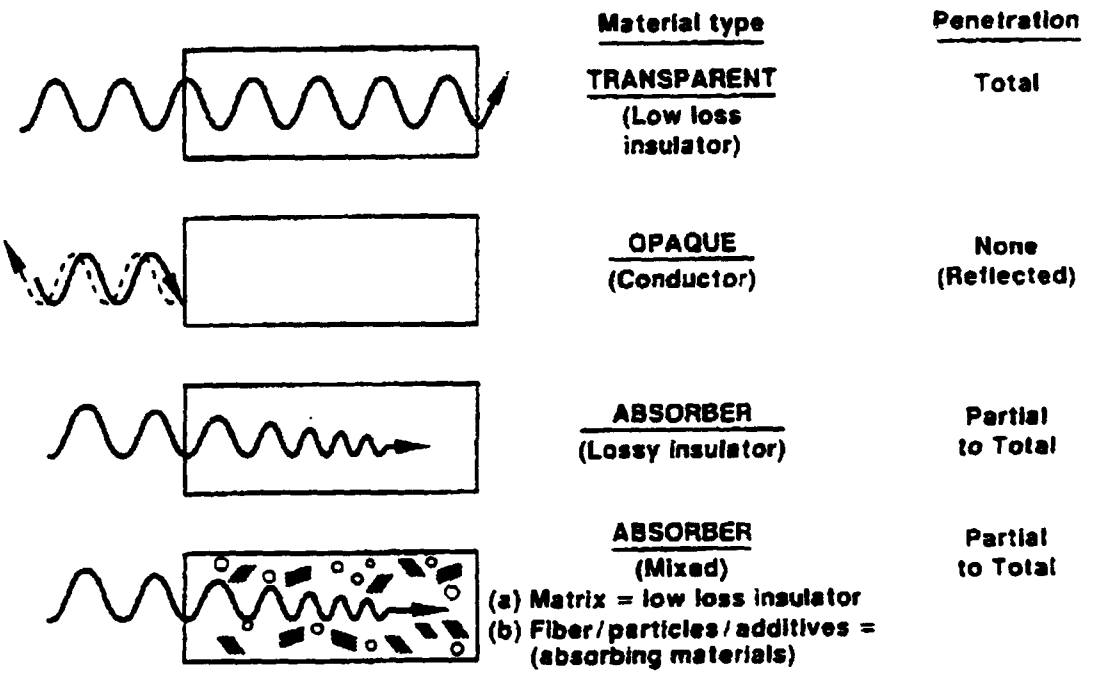

Figure 14: Materials classification based on microwave absorption [Ref. S4].

Materials can be divided into three categories according to their microwave properties (see Fig. 14). Materials with a very low loss tangent, e.g., fused silica, allow microwaves to pass through with very little absorption and are considered trarsparent, non-coupling, or non-absorbing

to microwaves. Materials with extremely high loss tangents, e.g., metals, reflect microwave radiation and are considered opaque to microwave energy. Materials with intermediate loss tangents, e.g., zirconia and silicon carbide, will readily absorb or couple with microwave energy [Ref. H3].

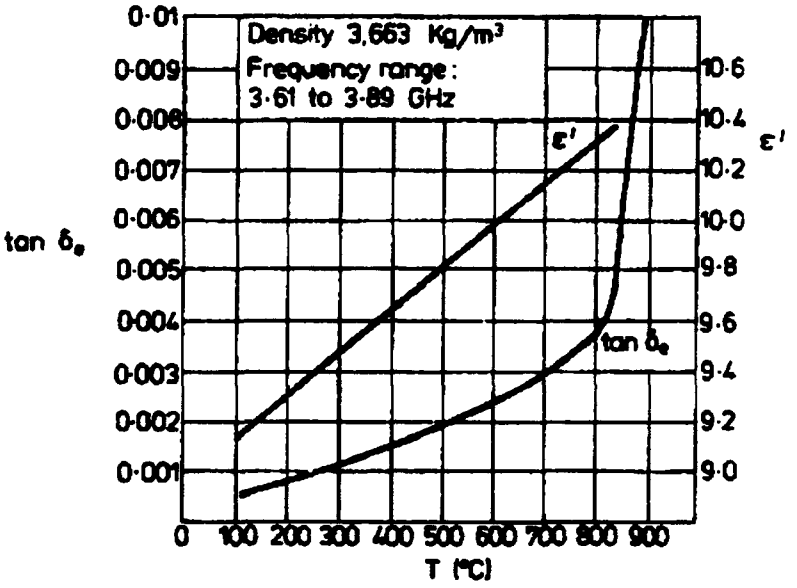

Figure 15: The loss tangent and dielectric constant for alumina as a function of temperature [Ref. B1].

For many low loss ceramics like alumina, the effective loss tangent is very low at room temperatures. Above a critical temperature, approximately 800 - 1000 Deg C for alumina (see Fig. 15), the loss tangent rises dramatically due to the increased ionic conductivity at the elevated temperatures resulting in enhanced coupling to microwave energy and increased heating [Ref. S1]. From equation 2, the effective loss tangent decreases with increasing frequency as shown in Figure 16.

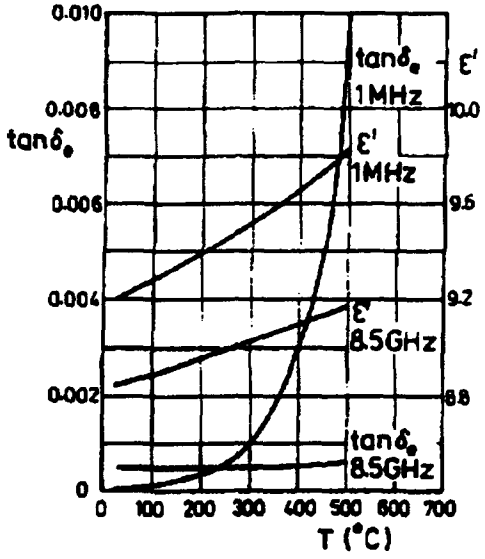

Figure 16: The effective loss tangent and dielectric constant for alumina 206 (95% alumina) as a function of temperature [Ref. B1].

3. Power Dissipation

A useful parameter is an estimate of the amount of power dissipated into a dielectric with a known effective loss factor.

For a high frequency electric field,

$$\mathbf{E} = \mathbf{E}_{max}\sin\omega\tau \qquad (3)$$

The polarization vector, P, which is out of phase with the electric field is then expressed as,

$$\mathbf{P} = \mathbf{P}_{max}\sin(\omega\tau-\phi) \qquad (4)$$

where ϕ accounts for the phase lag between E and P as shown in Figure 17. If **P** and **E** are in phase, ϕ is zero and the average power dissipated into the dielectric is zero.

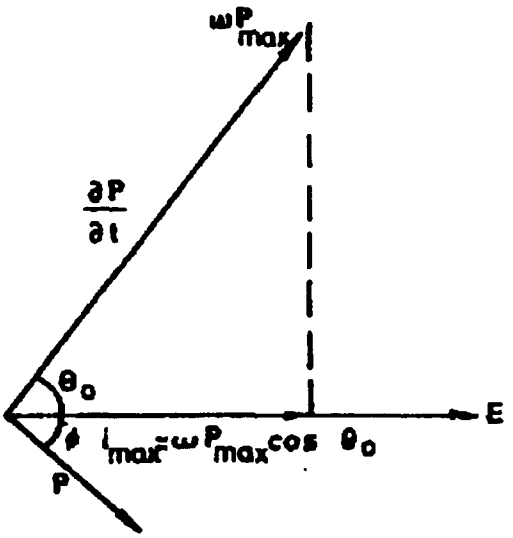

Figure 17: Phasor diagram showing the electric field vector, the polarization vector and the resulting current density [Ref. M7].

Power dissipated into the dielectric can be expressed as,

$$Power = E\frac{\delta P}{\delta \tau} = \frac{1}{2}E_{max}P_{max}\omega\,[\sin(2\omega\tau)\cos\phi + (1-\cos(2\omega\tau)\sin\phi] \qquad (5)$$

The average power dissipated can be expressed as,

$$P_{av} = \frac{1}{2}E_{max}P_{max}\omega\sin\phi = \frac{1}{2}E_{max}P_{max}\omega\cos\phi_o \qquad (6)$$

where $\cos\phi_o$ is the power factor.

Using the Pointing vector, $\rho = E \times H$, and Maxwells equations [Ref. M6], one can arrive at the power per unit volume as,

$$\frac{P_{av}}{V} = \omega \varepsilon_o \varepsilon''_{eff} E^2_{rms} \qquad (7)$$

A low-loss dielectric may require special microwave cavities or special enhancers to ensure that sufficient power is dissipated into the material.

Another expression for the average power per unit volume is,

$$\frac{P}{V} \propto Qf\varepsilon''|E|^2 \qquad (8)$$

where Q is the Quality Factor of a coupling system. Thus, high Q factors combined with high electric field strength produce very high heating rates [Refs. T2 and P1].

An alternative expression for power deposited in a dielectric subjected to microwave heating is given by the following formula:

$$Power = E\frac{\delta P}{\delta \tau} = (2\pi f \varepsilon') \left(\frac{E^2}{2}\right) Tan\delta_{eff} \qquad (9)$$

where, f = frequency.

It becomes apparent that the dielectric must have a large loss tangent and dielectric permittivity to achieve power absorption or alternatively, a low microwave coupling material may be assisted with higher frequency and greater electric field strength [Ref. M6].

4. Heating Rate

The rate of power dissipated and the heat capacity of the material determines the rate of temperature rise. Power dissipated results in a temperature rise according to the following relationship,

$$\mathbf{P} = \frac{Q_h}{\tau} = MC_p\left(\frac{\delta T}{\delta \tau}\right) \qquad (10)$$

substituting in for power, equation 7, the heating rate is obtained [Ref. T2],

$$\frac{\delta T}{\delta \tau} = \frac{\omega \varepsilon_0 \varepsilon''_{eff} f\, \mathbf{E}^2_{rms}}{\rho C_p} \qquad (11)$$

Microwave heating is better accomplished with higher effective loss factor (through the addition of additives and susceptors that readily couple with the microwave field), higher field strength, and possibly higher frequency (with the use of gyrotrons and klystrons).

Calculating the rate of temperature rise is not directly obtainable due to difficulties in determining the power dissipated. The rate of power dissipated is difficult to calculate for two reasons: first, very often the dielectric properties of the material being heated are not known as a function of temperature and density, and second, detailed information concerning the electric field in the microwave cavity and in the material being heated are not readily calculable. Once the material is introduced into a microwave cavity, it alters the absolute value of the magnitude of the electric field in the cavity and in the material [Ref. M6].

5. Penetration Depth

The process of depositing energy into the material, is limited by the depth of penetration of the electromagnetic field. As the electromagnetic energy penetrates into the interior of the material, it attenuates depending on the effective loss factor, of the material. This amount of absorption is quantified by the definition of penetration depth and is the distance into the material at which the electric field falls 1/e or 37% of its initial value [Ref. M6].

For an incident power, an expression for the attenuation factor, α is,

$$\alpha = \omega\left(\frac{\mu_o \mu' \varepsilon' \varepsilon_o}{2}\right)^{\frac{1}{2}}\left[\left(1 + \left(\frac{\varepsilon''_{eff}}{\varepsilon'}\right)^2\right)^{\frac{1}{2}} - 1\right]^{\frac{1}{2}} \qquad (12)$$

where,

μ_o = premeability of free space

μ' = real magnetic loss factor

The inverse of the attenuation factor is the skin depth, d_s [Ref. M6].

$$d_s = \frac{1}{\alpha} = \left(\frac{2}{\sigma\omega\mu_a}\right)^{\frac{1}{2}} \qquad (13)$$

where,

μ_a = absolute permeability

The depth of penetration, D_p is,

$$D_p = \frac{1}{2\alpha} = \frac{d_s}{2} \qquad (14)$$

Skin depth is more applicable to induction type heating where most of the power is dissipated at the surface, and heat transfer to the interior is by conduction aided by current density penetration. For microwave heating, power penetration depth is more applicable.

Table V: LOSS TANGENTS AND PENETRATION DEPTHS AT VARIOUS TEMPERATURES FOR HOT PRESSED BORON NITRIDE [Ref. B1].

T °C	ϵ'	$\tan \delta_e$	D
00	4.22	6×10^{-4}	7.
00	4.25	8×10^{-4}	5.
00	4.28	20×10^{-4}	2.
00	4.35	70×10^{-4}	0.
50	4.4	100×10^{-4}	0.

For solids, power penetration generally decreases with increasing temperature as shown in Table V. At frequencies below 100MHz, power penetration depth for alumina is in the order of meters. But, at microwave frequencies, penetration depth is much smaller, and coupled with high loss factors, the **Dp** may be of the order of a few cm, resulting in non-uniformities in temperature distribution for large samples.

Additionally, with an increasing loss tangent, the power penetration depth becomes smaller, leading to severe non-uniform heating and large thermal gradients characteristic of conventional surface heating techniques [Ref. P1]. Table VI shows the power penetration depth of various ceramics.

Table VI: Penetration Depths For Various Materials [Ref. B1].

Material	T °C	f MHz	ϵ'	ϵ''_e	tan δ_e	D_p m
Pyrolytic boron nitride	800	2450	3	2×10^{-4}		169
Calcium titanate	25	2450	180	2×10^{-3}		131
Steatite	25	2450	6	2×10^{-3}		23.9
Lime alumina silicate	25	2450	7	6×10^{-3}		8.6
Porcelain	25	2450	5	1.5×10^{-2}		2.9
Barium/strontium titanate	25	2450	2000	0.5		1.74
Barium titanate	25	2450	700	0.3		1.72
Hot pressed aluminium nitride	500	8500	9		4×10^{-3}	0.47
	700	8500	9		1.5×10^{-2}	0.12

E. MICROWAVE APPLICATIONS

Industry has forseen the possible advantage of microwave technologies faster processing times, uniform heating capabilites, and improved product qualities. Microwaves are extensively used in drying, joining, calcining, etc. (see Table VII). A large portion of research effort has been devoted to microwave-assisted ceramic processing such as sintering.

F. MICROWAVE APPLICATORS

A discussion of microwave radiation is not complete without introducing its integral interaction in a microwave cavity. This would not be the case if the wavelength of microwave radiation were very small, then the wave nature of the electromagnetic field could be neglected. The wavelengths

Table VII: MICROWAVE ENERGY APPLICATIONS IN CERAMIC PROCESSING [Ref. B1].

Drying	to accelerate the removal of moisture from green bodies.
Slip casting	to increase the casting rate; also includes accelerating the drying of moulds and ware.
Sol-gel processing	to reduce the number of processing steps involved in producing a sintered body from sol-gel technology.
Calcination	to accelerate the process; so far only superconducting systems and some electro-ceramics appear to have been studied.
Sintering	a wide range of ceramic and ceramic composite systems are currently being studied with a view to accelerating the process (and improving economics), and to generating novel microstructures.
Joining	to decrease time required to join ceramics and, possibly, to allow a greater range of ceramics to be joined. Both oxides and nonoxides are currently under investigation.
Plasma-assisted sintering	to use microwaves to generate plasmas to assist oxide sintering.
CVD	to use microwaves to decompose gaseous species which recombine to form thin films or powders.
Other applications	includes process control, clinkering of cement products, heating of optical fibre preforms, etc.

of infrared radiation used in radiant element heating are approximately .001 cm long, and is much smaller than most objects being heated.

In the case of microwave heating however, the wavelength is approximately 12 cm long, about the same range size of most microwave ovens. Even for large sample sizes, the wave nature of microwaves, their interactions inside oven cavities, and their influence in ceramic samples must be considered. Therefore scattering, diffraction, interference, and reflection and refraction phenomena associated with the wave-like nature of electromagnetic fields come into play [Ref. L1].

1. Standing Wave Patterns

In the microwave cavity, incident beams and reflected beams interact forming wave-like patterns. Incident and reflected beams are in continuous motion, but the resulting electric field pattern remains stationary and are referred to as standing waves. Standing wave patterns occur at discrete distances from reflecting surfaces. A maximum value in the standing wave occurs when the sinusoidal interactions of both incident and reflected beams combine, while interactions resulting in cancellations produce minimal values. This would produce hot and cold spots in microwave cavities were it not for mode stirrers to continually perturb the microwave field.

When an object is placed in the cavity, the fundamental standing wave patterns change due to changes in the reflection characteristics inside the cavity.

2. Modes

Incident beams in microwave cavities produce multiple reflections, and multiple three dimensional standing wave patterns, or modes. Typical microwave ovens contain a mixture of many patterns, and are referred to as multimode cavities. By allowing the microwave energy to reflect numerous times off the cavity walls a large number of cavity modes are excited, and power density becomes more uniform [Ref. K3]. By properly designing the dimensions of the cavity, a fundamental standing wave pattern can be produced, such a cavity is then single moded.

3. Tuned Applicators

The cavity containing the material to be heated is referred to as the applicator. Microwave applicators can be either single or multimode, tuned or untuned. Single and multimode cavities may both be tuned to produce a desired mode pattern. A cavity is considered untuned when individual mode resonances overlap to form a continuum and occurs when the wavelength of the microwave field is relatively large with respect to the cavity dimensions. Tuning is usually accomplished with the aide of a sliding short circuit plunger or variable aperture assembly which changes the dimensions of the cavity.

G. LIMITATIONS OF THE KITCHEN MIROWAVE OVEN

Typical commercially available microwave ovens are multi mode, untuned applicators, of approximately 1.2 to 1.5 cu.ft., configured with a continuous wave, 500 - 850 watt, magnetron operating at 2.45 GHz [Ref. M1]. These are acceptable design specifications for typical food processing applications, but are extremely limiting for serious microwave thermal processing of small low loss ceramic materials [Ref. Y1].

The field density of kitchen microwave ovens is very low, less than 1 kw/cu.ft. The field uniformity in the microwave cavity is also extremely low with severe field gradients causing numerous hot spots. To improve field uniformity and minimize the possibility of hot spot concentrations, a motorized turntable or mode stirrer is employed. A turntable is a platter that rotates food through the various hot spots. The mode stirrer is usually a 45 Deg section of aluminum plate with rounded edges, located in the microwave field and operates like a fan to continuously perturb the microwave field distribution.

Since the operating system is untunable, an improperly coupled condition exists between the non-receptive ceramic sample and the high power microwave source. The ceramic material absorbs only a portion of the microwave power delivered from the magnetron. The unabsorbed energy is reflected back to the source causing overheating of the magnetron until the thermal cut-off sensor, factory set at 140

Deg C, is activated. Continuous operation under these conditions could result in the degraded performance of the magnetron, leading to permanent damage.

Neither the frequency or the power output is adjustable on the kitchen microwave ovens. Power controls utilize a simple on/off duty cycle timer.

The advantage of commercially available kitchen microwave ovens is the cost. A typical kitchen microwave oven costs under $100.

H. RESEARCH QUALITY MICROWAVE OVENS

Research quality microwave ovens are very expensive starting at about $15,000 [Ref. G1]. They require a high quality, high voltage D.C. power source, an externally cooled microwave generator, a protection device that directs reflected energy away from the source to a dummy load (usually water) that absorbs the microwave energy and dissipates the heat to an external coolant.

Research quality microwave ovens are equipped to produce high microwave field densities. Using a coupling iris and a short circuit plunger assembly, they can be tuned for maximum energy absorption and minimum reflected losses. The microwave generator is equipped with a protection device to maintain uninterrupted operations even under highly reflected power conditions to minimize the possibility of overheating.

IV. PREVIOUS WORK ON MICROWAVE INTERACTION AND PROCESSING OF MATERIALS, PARTICULARLY CERAMICS

The possibility of utilizing microwave energy as a heating source was discovered as early as the 1940's after the development of radar for WWII. It was the utilization of the magnetron as a pulse generator that advanced the capability of the radar. After the war, peacetime profitable use of radar and the magnetron was encouraged by government and industry.

A. HISTORICAL BACKGROUND

A lack of understanding of the fundamental nature of how microwaves interact with matter led von Hippel and his team at MIT to begin investigating how oxide materials interact with microwave radiation and how the loss characteristics of these materials vary as a function of microwave frequency. Later, in the 1950's Von Hippel compiled the first tabulation of dielectric measurements for various materials; pure organic and inorganic liquids solids and mixtures over a wide frequency range (10 Hz -10 GHz) [Ref. V1]. Though most of the results were obtained at room temperature some were at higher temperatures up to 200 degrees centigrade.

In the 1960's, interest in developing microwave energy as an economical heating source declined until the 1970's when the escalating cost of fossil fuels, oil and gas, promoted a

resurgence in developing a more efficient means of heating [Ref. B4]. However, in the 1960's Westphal and Inglesias [Ref. I1], acquired dielectric data on high temperature solid materials including oxides, nitrides, and silicates. While Tinga [Ref. T4] investigated how certain oxides developed reaction cavities and absorbed energy in a microwave field. Ford and Pei [Ref. F2], used a multimode microwave oven with two 800 W, 2.45 GHz magnetrons in with a mode stirrer and studied a variety of oxides and non-oxide materials and concluded that sample size was important for low loss materials. Increasing sample size gave higher heating rates.

In the 1970's Stuchly and Hamid [Ref. S2], experimentally confirmed the inverse temperature profile for a broad range of material systems. Sutton [Ref. S6] investigated the drying and firing of large castable alumina ceramics. Brooks [Ref. B6] showed that rapid sintering led to improved ceramic microstructures and high density with the development of finer more uniform grain structure. Also, von Hippel, again at MIT, obtained valuable information on the frequency and temperature dependence of the dielectric properties of a large number of ceramic material both oxides and non-oxides. Westphal [Ref. W2], at the Air Force Materials Laboratory, obtained a more extensive collection of data on over a thousand different types of materials, not only ceramic but also inorganic and organic material. They investigated the dielectric properties not only as a function of microwave frequency but also as a

function of temperature. The frequency range was extended to 25 GHz and temperatures up to 1000 Deg C.

In the 1980's, Meek [Refs. M4 and M5] showed significant differences between conventional thermal processing and microwave processing of glasses, ceramics and composites. They observed material transport, rapid sintering, and different microstructure for various ceramic materials heated at 2.45 and 6 GHz. To sinter low loss ceramics at 2.45 GHz Meek suggested the use of various susceptor materials and a second or primary phase material which acts as a crack inhibitor upon sintering.

In the 1980's Harmer and Brook [Ref. B6], developed a theory which predicts that rapid sintering will result in a finer grained microstructure. The theory applies to all rapid sintering techniques including microwave sintering. The theory of rapid sintering is based on the simple assumption that both densification and grain growth are thermally activated processes and that the activation energy for grain growth is lower than that for densification. Kimrey [Ref. K3] demonstrated the ability to sinter large complex shaped ceramic components due to the volumetric heating effects of microwave energy.

In 1987, Blake and Meek [Ref. B7] investigated a second phase which aided the coupling of a green body with incident microwaves providing the additive aids in the coupling and densification process is not detrimental to the properties of

the sintered body, i.e., leaving residual glassy grain boundary phases. Johnson [Ref. J4] reported the successful sintering of alumina specimens at 1500-1800 Deg C and at a rate of 2 mm/min. Sintering temperature was reached in about 10 minutes using 250 W at 2450 MHz in a rectangular cavity. The resulting microstructure had extremely fine average grain size (0.78 um). Brook [Ref. B6] showed that as a direct result of rapid heating or "fast firing", (>400 Deg C/min), alumina could be sintered to very high densities (>99%) with grain sizes less than 1 um when conducted under optimal conditions.

In 1988, Harrison [Ref. H2], compared the microstructure of PZT and PLZT pellets after microwave sintering and conventional sintering. A similar density but smaller grain size was obtained with microwave sintering, but required only 12 minutes as opposed to 60 minutes and only 5% of the energy needed by conventional sintering. Ho and Harker [Ref. H3], demonstrated that as a function of temperature, the dielectric constant depended only on the material's crystalline lattice properties. Other factors such as microstructure and purity are only secondary contributors, while dielectric losses, on the other hand, are dependent on microstructure and grain boundary properties. This explained the rise in loss tangents for polycrystalline materials over the same single crystal material.

B. TEMPERATURE MEASUREMENTS

An accurate indication of instantaneous temperature measurements without electromagnetic field interference or microwave exposure hazards will always be of major concern.

Thermocouples have been predominantly used because of their simplicity and accuracy. Thermocouples, however, require electrical shielding and thermal insulation to properly function at elevated temperatures produced in microwave sintering. A bare thermocouple would arc severly and possibly melt during the sintering process. Thermocouples can be thermally insulated in a ceramic tube which is then electrically shielded with a sheath like molybdenum. Operating conditions of the thermocouple and sheath must be considered to reduce the effects of oxidation and performance degradation.

Sheath diameter influences temperature response times and microwave field concentration effects. A smaller diameter produces a faster response time but also a larger field concentration leading to severe arcing. A 1/8-in. diameter Molybdenum-sheathed type-C thermocouple produced a response time of ~30 secs without electrical discharge in an Ar-1%N_2 atmosphere [Ref. J1].

Even with electrical shielding and insulation, Tinga [Ref. T1], suggested utilizing brief off periods to obtain thermocouple measurements to prevent possible microwave interference with thermocouple temperature measurement

devices. Fang [Ref. F1] noticed that microwave interference occured at low temperatures, but once ceramic coupling commenced, temperature readings stabilized. Initial temperature readings were thus recorded during momentary power supply off periods.

C. UTILIZING ADDITIVES

Meek [Ref. M4] used a variety of additives to achieve microwave sintering. The results indicated that SiC markedly improves the hardness of alumina and paint-grade CaO stabilized ZrO_2. Nitrates and glycerol were shown to be very effective sintering aids in microwave processing of alumina-silicon carbide whiskers. Additions of small amounts of second-phase material to common oxide materials enhanced the densification.

Holcombe [Ref. H1] investigated the mechanical and physical properties of microwave sintered paint grade Yittria containing 2 wt% zirconia versus commercially available material of similar composition. The microwave processed material had a modulus of elasticity between 77 - 206.5 GPa as compared to 150.5 GPa for the commercial material. The thermal shock resistance of the microwave processed material was superior to the commercial material. This was attributed to the high microwave sintered material possessing disconnected, spherical porosity while the commercial material contained connected, non-spherical pores.

D. SUSCEPTOR MATERIALS

Susceptors are materials that exhibit high losses at low temperatures. Ferrites, zirconia, and silicon carbide have long been recognized as extremely effective microwave energy absorbers [Ref. S1]. For small non-receptive materials, its advantage as a microwave coupler became apparent since the 1970's [Ref. M3].

Krage [Ref. K4] in 1981 used ferrites in a microwave-absorbing susceptor base plate to support green magnets in order to achieve sintering results.

Wilson and Kunz, [Ref. W1] when sintering yittria stabilized zirconia (Y-PSZ), utilized a disc shaped suceptor made of silicon carbide. Sintering of green bars was achieved at 2.45 GHz. By viewing the reflections off darkened glass during sintering, they observed that sintering initiated with an outward bowing of the sample's edges, followed immediately by small cracks. The center glowed and shrunk, with continual heating. The glowing area radiated outward until the entire sample completed sintering. Theoretical densities of 95% were obtained in considerably less time than conventional sintering.

Janney and Kimrey at ORNL [Ref. J2] discovered it was difficult to produce crack free parts in a multimode microwave furnace due to non-uniformities in the microwave field. Since dielectric properties increased rapidly with temperature, it produced hot spots in the parts which led to differential

sintering and subsequent cracking. To produce crack free sintered parts, a "picket fence" apparatus employing silicon carbide rods to provide direct and indirect microwave heating was used. This eliminated severe differential heating, lowered the sintering temperature and resulted in finer grain sizes and extremely high theoretical densities.

E. HIGHER FREQUENCIES

Increasing frequency is an alternative to utilizing susceptors or additives. With higher frequencies, greater power is deposited into the sample which increases the possibility that very low-loss materials may couple. Increasing frequency also increases field uniformity for a more even distribution of heating. The disadvantage of higher frequencies is that penetration depth is decreased to the point of approaching conventional heating methods.

Kimrey and Janney [Ref. K2] used a 200 kW continuous wave gyrotron operating at 28 GHz coupled to a large, 76 cm Dia. by 100 cm long, untuned cavity to sinter large, 1000 g or more, ceramic components. This resulted in greater than 98% theoretical density over much of the sample volume.

Meek [Ref. M5] sintered high purity, submicron alumina powders to greater than 95% theoretical density in about 6 minutes at 1700 Deg C with a 60 GHz microwave source. Even with rapid sintering times, significant grain growth occured, in the order of 5 μm, with pockets of incompletly densified

material of original powder morphology observed. This indicated that inhomogeneous coupling of the microwaves occured and was attributable to the decreased penetration depth associated with higher microwave frequencies.

V. SCOPE OF THE PRESENT WORK

Based on the literature review, microwave processing appears to be a promising technique when applied towards the thermal processing of ceramic powders.

The purpose of this work was to investigate the possibility of utilizing a commercially available kitchen microwave oven for sintering ultrafine alumina powders with and without sintering aids. Preliminary results from the experiments conducted are reported.

A. EXPERIMENTAL APPARATUS

The experimental apparatus as shown in Figure 18, consists of an argon cylinder, glove box, microwave oven, sample, water bottle, and data acquisition system.

A sealed plexiglass glove box was used to contain the microwave oven in an inert atmosphere. An inert atmosphere, provided by the argon gas, was required to prevent oxidation degradation of the molybdenum sheathed W/W-Re thermocouple probe (Omega™, Type-C, 1/8" Dia.) and to prevent oxidation of the graphite powder susceptor material used to surround the sample. Containing the entire microwave oven in an inert atmosphere and not just encapsulating the crucible and thermocouple in a container filled with argon gas, ensured that the crucible received unattenuated, direct exposure to

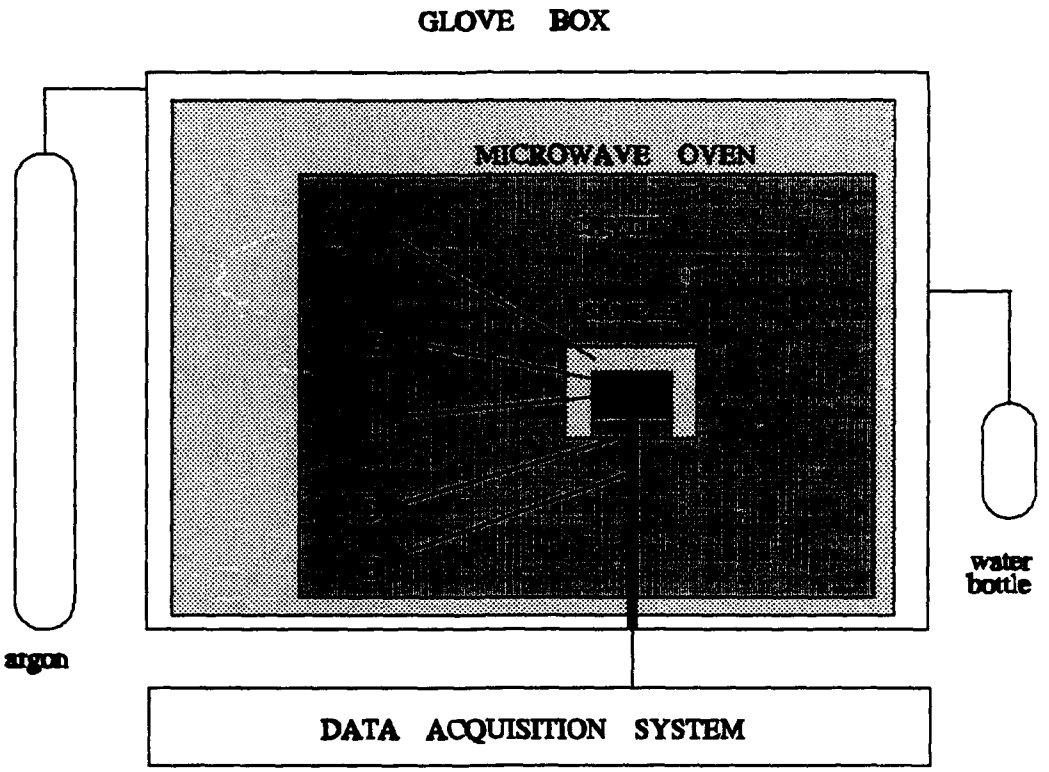

Figure 18: Schematic diagram showing the experimental apparatus with A. mullite crucible, B. susceptor material (carbon or alumina and carbon), C. pellet, D. Fiberfrax™ insulating board, and E. thermocouple.

microwave radiation without the encapsulating material absorbing some of the microwave energy, heating and possibly melting. The glove box was also designed to permit transferring material in and out of the inert atmosphere, access to the microwave oven control panel, and manipulation of the sample and surrounding insulation without disrupting the integrity of the seal.

The argon gas exited the glove box through a plastic 1/2" Dia. tube submerged at a depth of 1" in a bottle filled with water. A small flow of argon bubbling from the plastic tube provided positive visual indication of the glove box's ability to maintain a seal and to prevent backflow of air into the box. When the experimental run was completed, the argon flow was terminated, and the sample was allowed to cool to room temperature.

The household microwave oven was a Quasar Model MQS0803W, manufactured by Matsushita Cooking Appliance Corporation. Behind a touch-sensitive control panel located to the right of the microwave cavity was a 750 W continuous wave magnetron manufactured by Panasonic Corporation. An L-configured, rectangular-shaped, waveguide directed microwave radiation to the bottom of the microwave cavity. The oven utilized a motor driven mode-stirrer located at the outlet of the waveguide to continuously perturb the microwave radiation as it entered the microwave cavity. The mode stirrer was concealed under a microwave transparent square base plate near the bottom of the microwave cavity.

To allow temperature measurements without interfering with the operation of the mode stirrer, the thermocouple was inserted through the top of the microwave cavity. The microwave oven was then turned upside-down to permit the sample to rest solely on the probe tip thus, the sample required no additional supporting material which could

possibly absorb microwave energy and acquire elevated temperatures, or reflect some of the microwave energy away from the bottom of the sample.

The microwave cavity was lined with three 1" thick, layers of Fiberfrax™ insulating blanket. The remaining volume immediately surrounding the crucible was thoroughly packed with Fiberfrax™ insulating bulk fiber. Both the insulating blanket and bulk fiber were composed of relatively microwave transparent material 72% alumina and 27% silica.

A cylindrical shaped, mullite, crucible 19 mm (ID), 25 mm (OD), 26 mm high with a bottom thickness of 8 mm, was used to contain the sample material.

Millivolt output information from the thermocouple were obtained by a Hewlett Packard (HP) 3852A Data Acquisition System. A HP 9153A computer system converted digitized millivoltage information to temperatures utilizing a 5th order polynomial (provided by the National Bureau of Standards).

B. EXPERIMENTAL PROCEDURE

1. Powdered materials and their processing

For this study, 0.05 μm (mean particle size) alumina polishing powder (100% purity, Buehler Ltd) and 0.02 μm (mean particle size) alumina powder (99.99% purity, Johnson Matthey Products) were used. The particle and aggregate sizes that comprise the 0.02 μm powder are given in Table VIII. Scanning electron micrographs of the original powder are shown in

Table VIII: SIZE DESCRIPTION OF THE 0.02 μm ALUMINA POWDER.

Description	Volume	Size (micron)
Particles	100%	0.01-0.02
Aggregates	100%	<4
	50%	<0.05
	25%	<0.03

Figures 19 and 20. When compacting the 0.05 μm powder neither sintering aid, binder material, nor lubricant were added. The 0.05 μm alumina pellet acquired sufficient strength without a binder addition to permit handling of the green product.

For compacting the 0.02 μm powder, 10 wt % CaO as a sintering aid, 2 wt % Polyvinyl alcohol (PVA) as a binder, and 1 wt % Polyethylene glycol (PEG) as a lubricant were added. For powder sizing and proper mixing, a ball milling device was employed utilizing a 4" Dia. cylinder and 1/2" Dia. spherical grinding media made of teflon to prevent contaminating the powders. An initial attempt at dry milling the combined materials resulted in the powder caking and thickly lining the inside of the rotating cylinder as well as the grinding media thus preventing a free-falling flow of materials that encourage proper mixing and particle sizing.

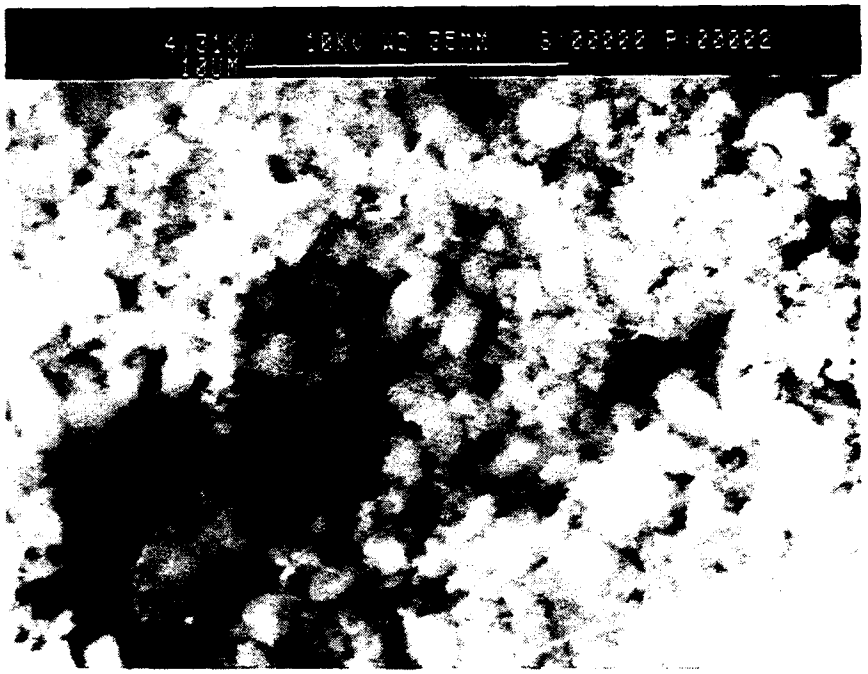

Figure 19: Scanning electron micrograph showing the aggregates which comprise the 0.02 μm alumina powder.

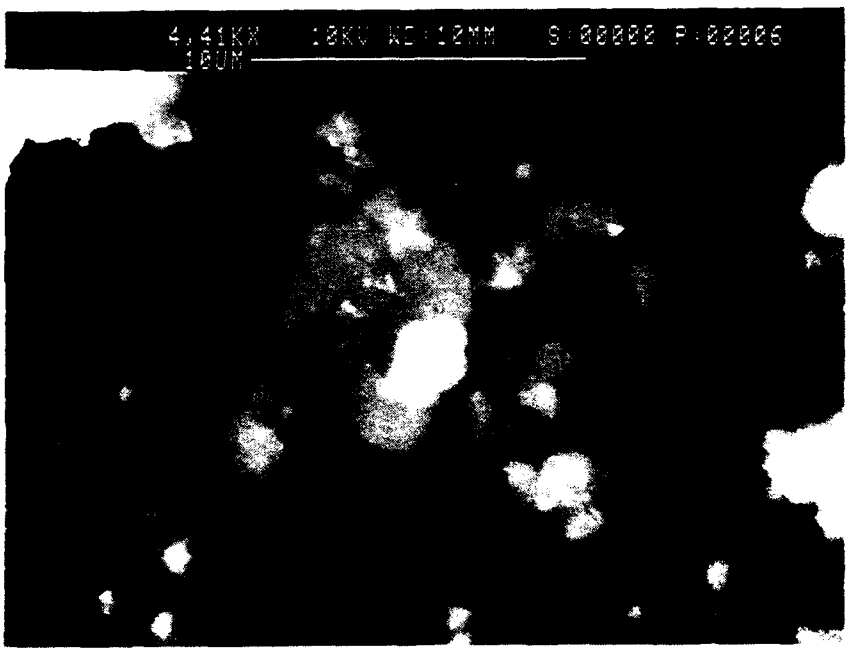

Figure 20: Scanning electron micrograph showing the 0.05 μm alumina powder.

Consequently, the combined materials were wet-milled with ethyl alcohol in a ball milling device for 16 Hrs at high speed then dried. The milling and compaction conditions for the different samples are shown in Table IX.

Table IX: VARIATIONS IN SAMPLE PARTICLE SIZE, COMPACTION PRESSURE, SURROUNDING MATERIAL AND COMPOSITION.

Sample Number	Particle Size (μm)	Compaction Pressure (MPa)	Surrounding Material	Sintering Aid	Binder Addition	Lubricant
1	0.05	200	Graphite	None	None	None
2	0.02	50	Graphite	10 wt% CaO	2 wt% PVA	1 wt% PEG
3	0.02	50	Alumina	10 wt% CaO	2 wt% PVA	1 wt% PEG
4	0.02	200	Graphite	10 wt% CaO	2 wt% PVA	1 wt% PEG

For all samples, approximately 0.5 g of powder was uniaxially compressed, in a simple punch and die device with a tool steel insert, at 50 or 200 MPa using a Baldwin™ hydraulic press to produce pellets approximately 13 mm in diameter and 3 mm thick.

2. Susceptor and relationship to alumina pellets

The bottom of a mullite crucible was filled with a layer of susceptor material composed of graphite powder (Asbury Graphite Inc.) which was loosely packed to a thickness of approximately 3 mm. The pellet was placed on top of the compacted graphite powder and additional powder was added to

sufficiently cover all surfaces of the pellet and packed again. A final thickness of 3 mm of graphite powder was obtained on all sides of the pellet. Graphite powder was used as a susceptor material because of carbon's ability to readily couple with microwave radiation. By surrounding the alumina pellet with graphite powder, it would by conduction raise the pellet to temperatures in excess of 1000 Deg C, above the critical temperature of the alumina pellet to initiate coupling with the microwave radiation. Once coupling commenced, the alumina pellet would readily absorb microwave energy and rapidly heat to sintering temperatures.

Because graphite could possibly react with the sample to produce undesirable carbon products, a layer of alumina powder separated the pellet from the graphite powder. For those pellets surrounded first by alumina powder and then graphite powder, the bottom of the mullite crucible was lined with graphite powder to a thickness of 3 mm and compacted as before, then a layer of 0.02 μm alumina powder was placed on the graphite powder and also compacted to a thickness of 3 mm. The pellet was placed on the alumina powder layer and additional alumina powder was added to cover all sides of the pellet, then compacted again. A thickness of approximately 3 mm of alumina powder surrounded all sides of the pellet. Finally a layer of graphite powder was placed on top and compacted to a thickness of approximately 3 mm. This resulted in a sandwich composed of graphite-alumina-graphite wafers.

The remaining volume of the crucible was capped with a layer of Fiberfrax™ insulating board until flush with the top surface of the crucible. A 1/8" diameter spare thermocouple probe was inserted through the fiberboard so as to be in contact with the pellet, then removed. The crucible was inverted, placed in the microwave oven and suspended on the thermocouple probe (already connected to the data acquisition system) through the pre-existing hole. Fiberfrax™ insulating bulk fiber was thoroughly packed between the crucible and the Fiberfrax™ insulating blanket lining the rest of the microwave cavity. The front face of the microwave cavity was lined with additional insulating blanket and the microwave door was closed. Fiberfrax™ insulating blanket was used to protect the microwave cavity from the effects of the elevated temperatures obtained by the sample. Fiberfrax™ insulating bulk fiber was used to surround the crucible thus reducing heat loss due to convection.

3. Operation

A sufficient flow of argon was admitted into the glove box, to replace the existing atmosphere with argon gas. After 5 - 10 minutes of purging, the microwave oven was set to run at high power (continuous magnetron operation) for time settings greatly exceeding desired sintering times. Accurate time keeping was performed by the data acquisition system. Both data collection and microwave operation were initiated

simultaneously. The argon flow remained throughout the sintering operation.

When sintering times were completed, microwave operations were terminated, the sample was quickly removed from the microwave cavity and placed on a ceramic tile, situated inside the glove box, and allowed to cool to room temperature. After 5 - 10 minutes of cooling the argon gas flow was terminated.

C. RESULTS AND DISCUSSION

For the 0.05 μm alumina powder compressed to 200 MPa and surrounded by graphite powder (Sample #1), temperatures above 1400 Deg C were reached with an initial temperature rate of approximately 75 Deg C/sec (Fig. 21). The maximum temperature obtained was 1500 Deg C. In Figure 21, the sinusoidal behavior observed after reaching the maximum temperature may be due to the magnetron's varying performance.

The optical micrograph showed sintering localized to less than half of the pellet surface (Fig. 22). The darkened areas were where the graphite powder adhered to the pellet surface. This sintered area appeared to be concave shaped and nearly circular in area. Note the glassy portion at the bottom left of the sintered area. Under the scanning electron microscope at low magnification this area appeared feature-less. It was difficult to obtain an EDX analysis of the area. Scanning electron micrographs of various areas of the surface showed

sintering at various stages (Figs. 23 - 25). Different morphologies appeared to be randomly scattered throughout the surface making it difficult to obtain a representative map of the surface. Figure 23 showed powder particles coalescing into aggregates about 4 μm in size during sintering. Figure 24 showed more advanced stages of sintering, while Figure 25 appears almost fully dense with surface pores becoming almost circular. The appearance of the sample in Figure 25 suggest that some melting may have also taken place. However, an EDX of the sintered area and non-sintered area indicated that only alumina was present in Sample #1, and therefore melting is unlikely to have occured at the maximum temperature achieved. A scanning electron micrograph of the sample interior (i.e., the cross-section) showed areas of partial sintering as well as fully dense areas (Figs. 26 and 27).

The fully dense regions contained distinct circular pores and the less dense regions exhibited high porosity. The two regions were adjacent to one another, with a crack separating them. It is possible that as the sintered region became more dense, it contracted and pulled away from the less dense region. Why the two widely degreed regions of densification formed adjacent to one another instead of a gradual transition from less dense to fully dense is not understood, but may be due to a large thermal gradient that separated the two regions.

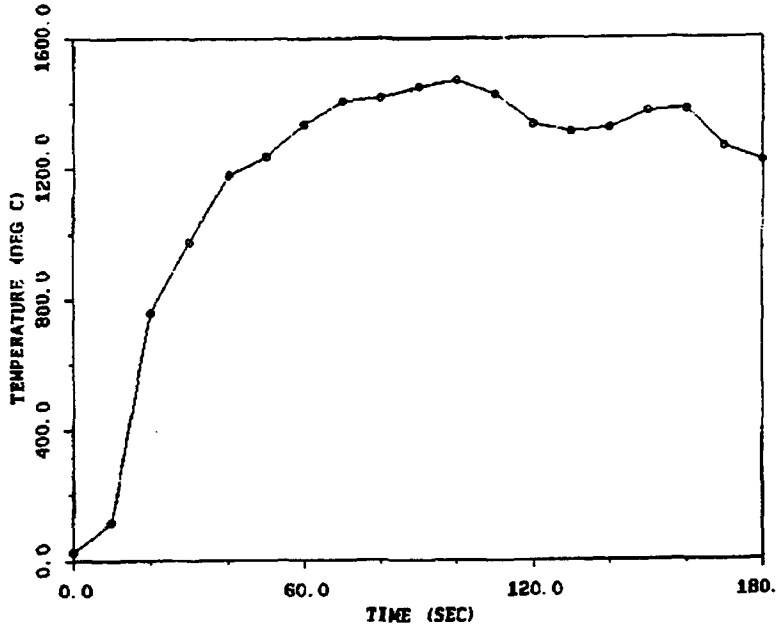

Figure 21: Temperature plot of the 0.05μm alumina powder, compressed to 200 MPa and surrounded by graphite powder (Sample #1).

Figure 22: Optical micrograph showing sintered and glassy region (Sample #1).

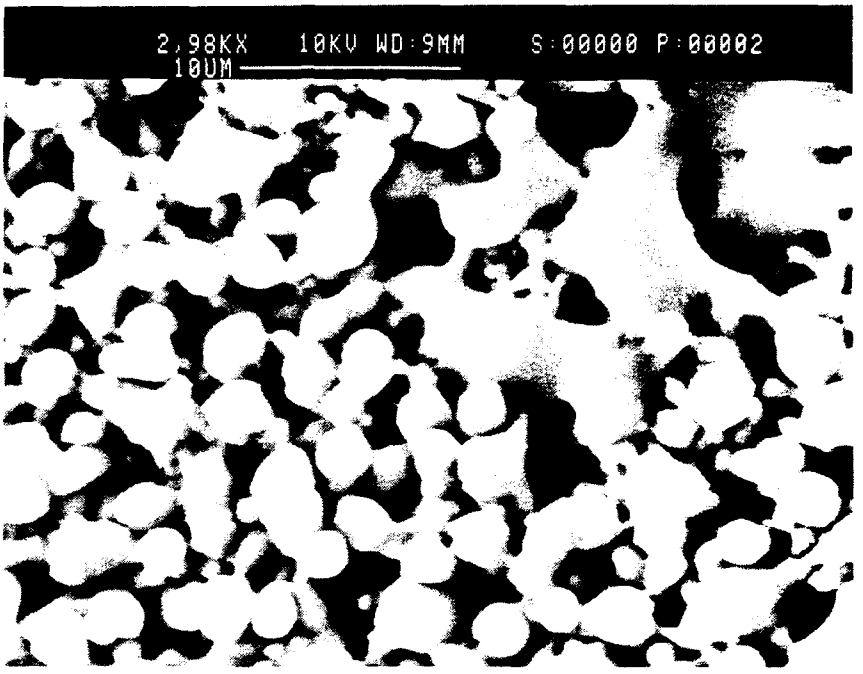

Figure 23: Scanning electron micrograph showing surface morphology (Sample #1).

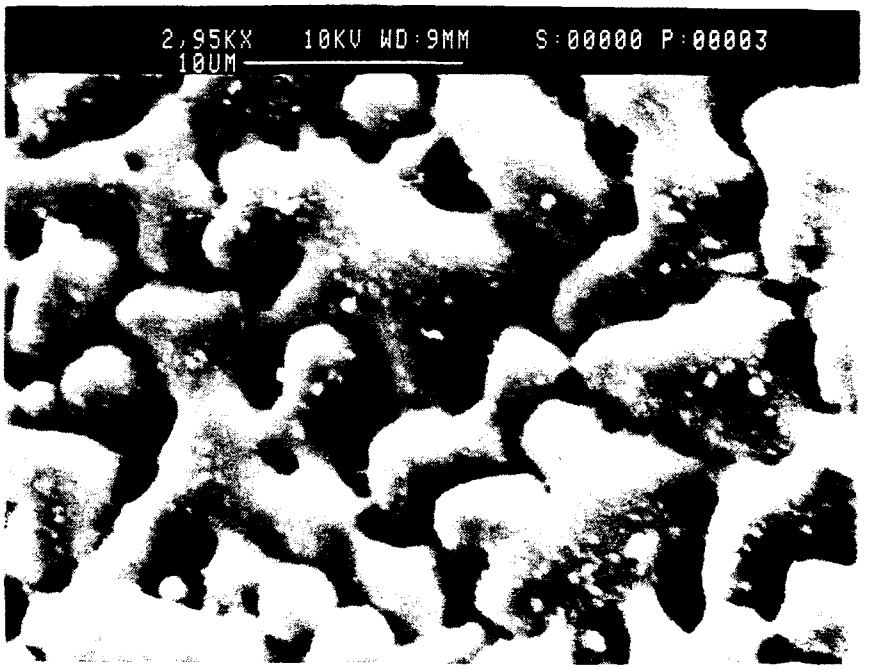

Figure 24: Scanning electron micrograph showing surface morphology (Sample #1).

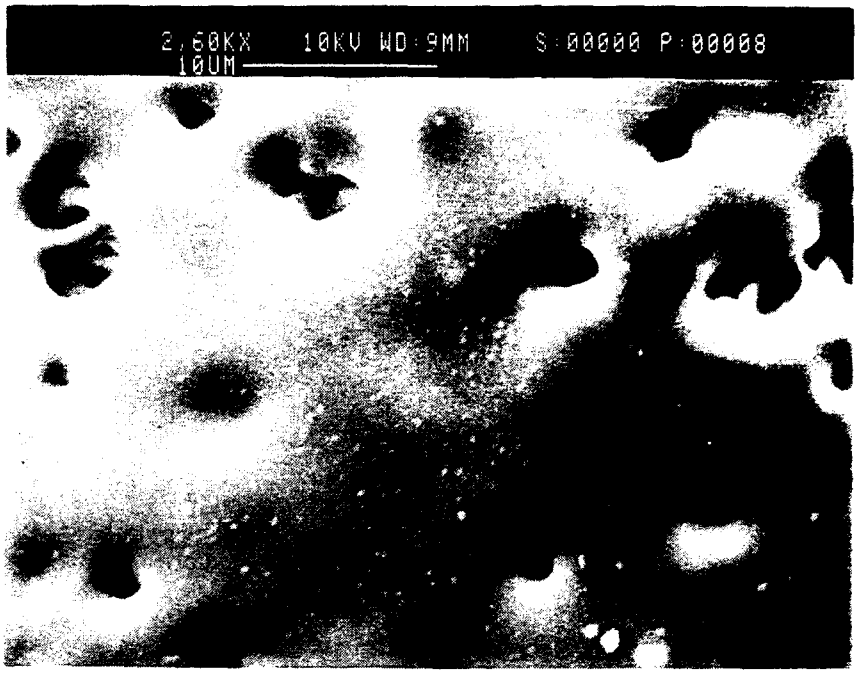

Figure 25: Scanning electron micrograph showing surface morphology (Sample #1).

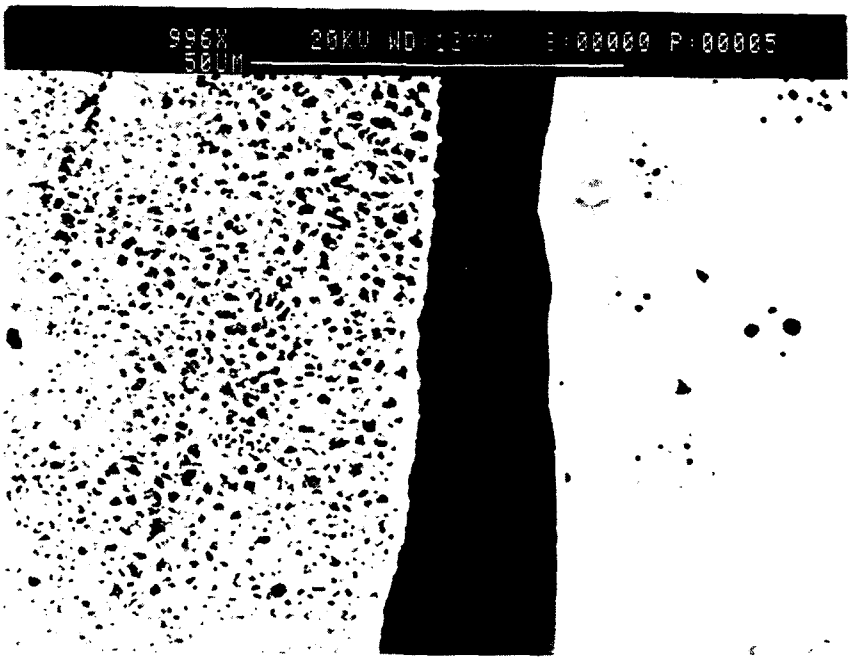

Figure 26: Scanning electron micrograph of the interior showing partial and fully dense regions (Sample #1).

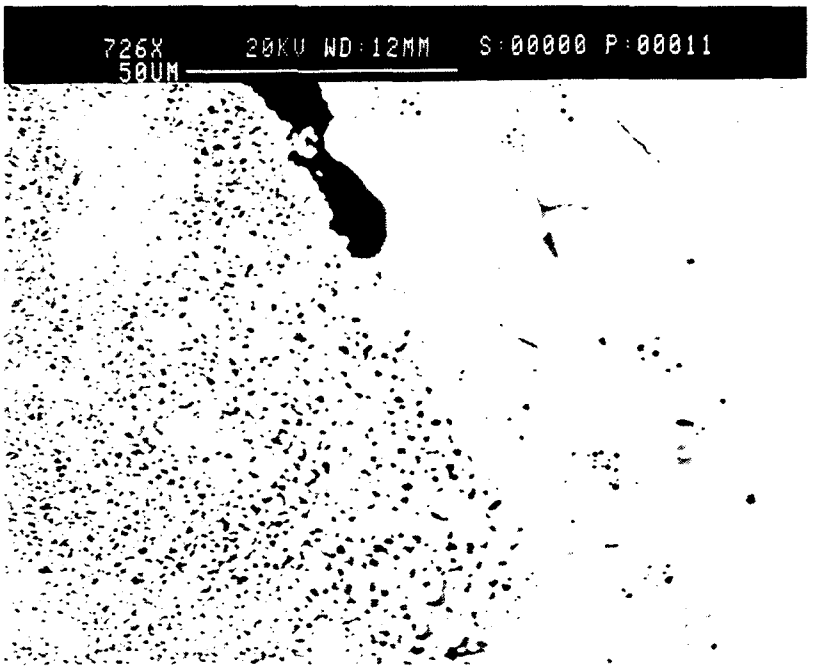

Figure 27: Scanning electron micrograph of the interior showing partial and fully dense regions (Sample #1).

For the 0.02 μm alumina powder, compressed to 50 MPA and surrounded by graphite powder (Sample #2), temperatures above 1500 Deg C were reached (Fig. 28).

The maximum temperature rate obtained was 55 Deg C/sec. The maximum temperature obtained was 1580 Deg C. The large peak and subsequent valley at the end of 50 seconds may be due to a power-off cycle in the magnetron that either occurs normally at the end of 50 seconds or abnormally due to magnetron ouput difficulties. The corresponding valley was possibly due to some convection losses even with the Fiberfrax™ completely packed around the crucible. An alternative possibility is that at approximately 1400 Deg C, the alumina pellet couples with the microwave energy and

acts like a heat sink absorbing a tremendous amount of energy before sintering.

The optical micrograph showed localized sintering (Fig. 29). The surface appearance was again similar to the optical micrograph of Sample #1 (Fig. 22) with the darkened areas due to carbon adhering to the sintered surface.

A scanning electron micrograph of the surface near the outer edge of the pellet showed little sintering had occured (Fig. 30), while the center of the pellet showed indications of sintering (Fig. 31).

A sketch of the interior portion of Sample #2 is shown in Figure 32. Scanning electron micrographs of the left half of the sample are shown in Figures 33, 34, and 35.

Scanning electron micrographs of the right half of the sample are shown in Figures 36, 37, and 38. Good sintering appears to be confined to regions in the vicinity of the thermocouple probe and extending to the interior of the sample. The 1/8" diameter probe may be concentrating the microwave field at the probe tip resulting in greater power dissipation closer to the probe.

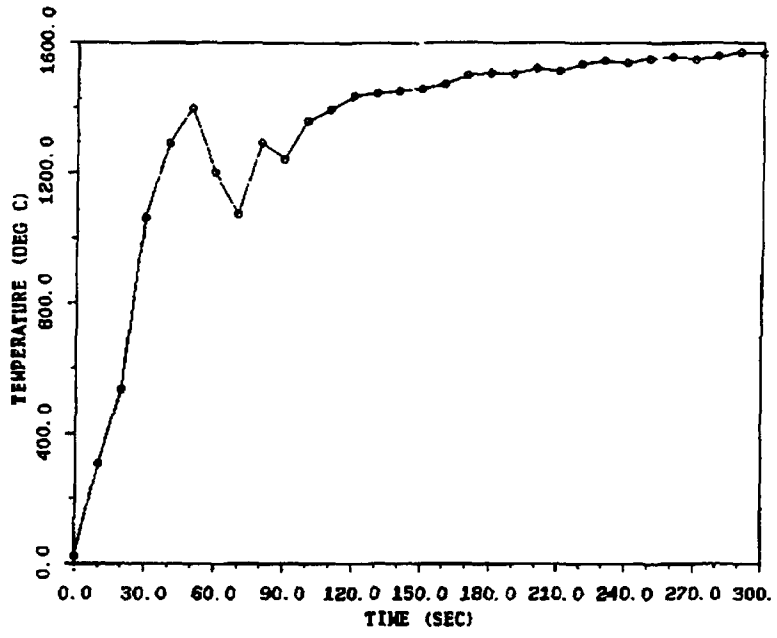

Figure 28: Temperature plot of the 0.02μm alumina powder, compressed to 50 MPa and surrounded by graphite powder (Sample #2).

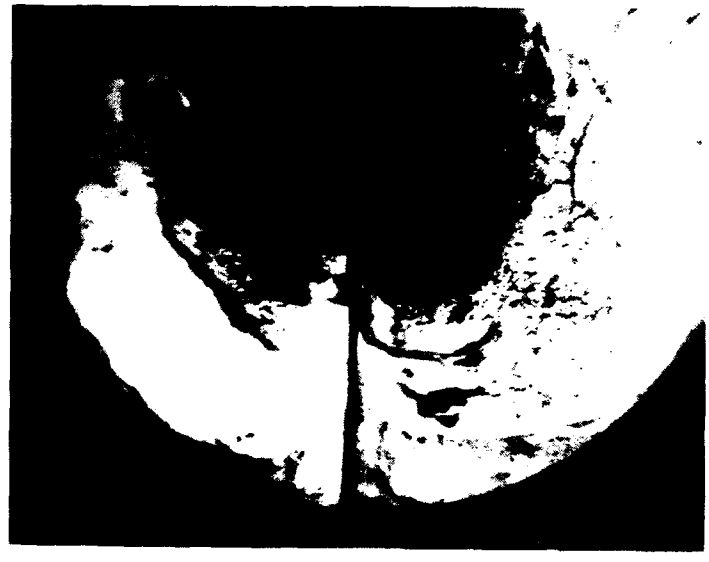

Figure 29: Optical micrograph showing localized sintering near the center of pellet (Sample #2).

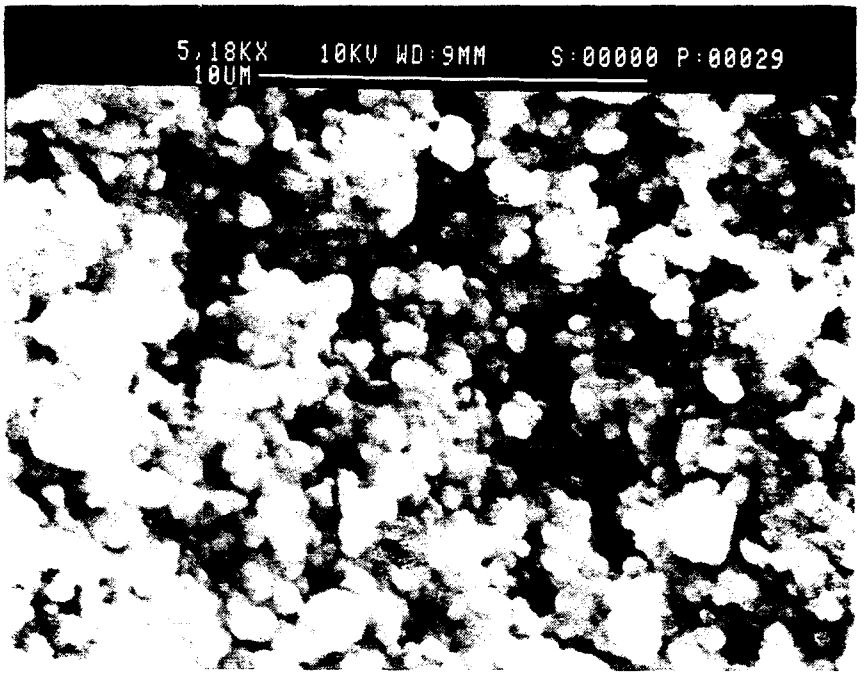

Figure 30: Scanning electron micrograph of the surface near pellet outer edge showing little sintering had occured (Sample #2).

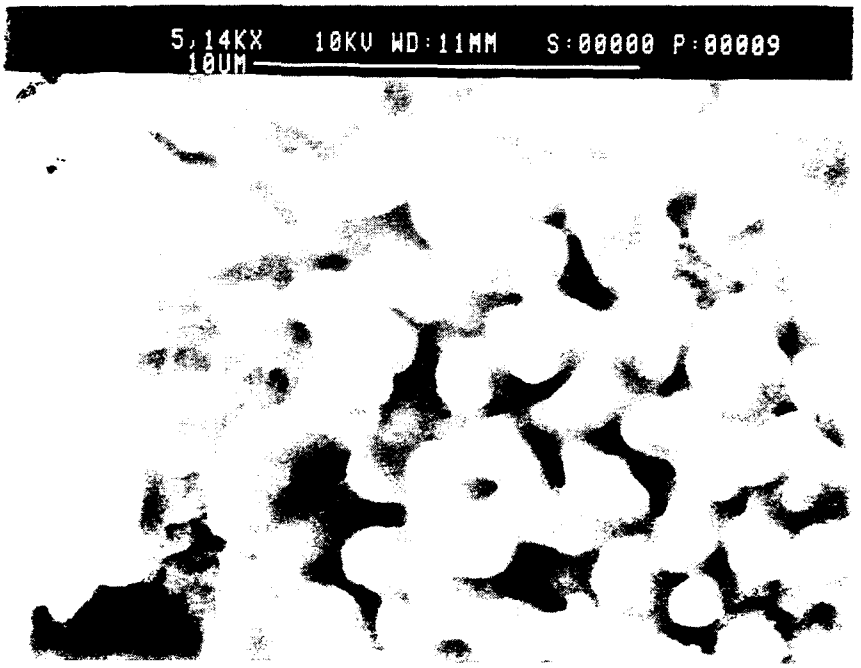

Figure 31: Scanning electron micrograph of the surface showing sintered aggregates near the center of the pellet (Sample #2).

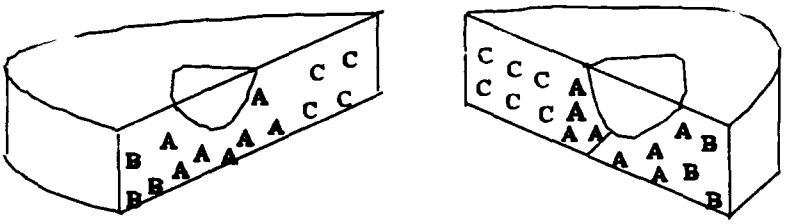

Figure 32: Sketch showing the location of represented areas as seen under the scanning electron microscope.

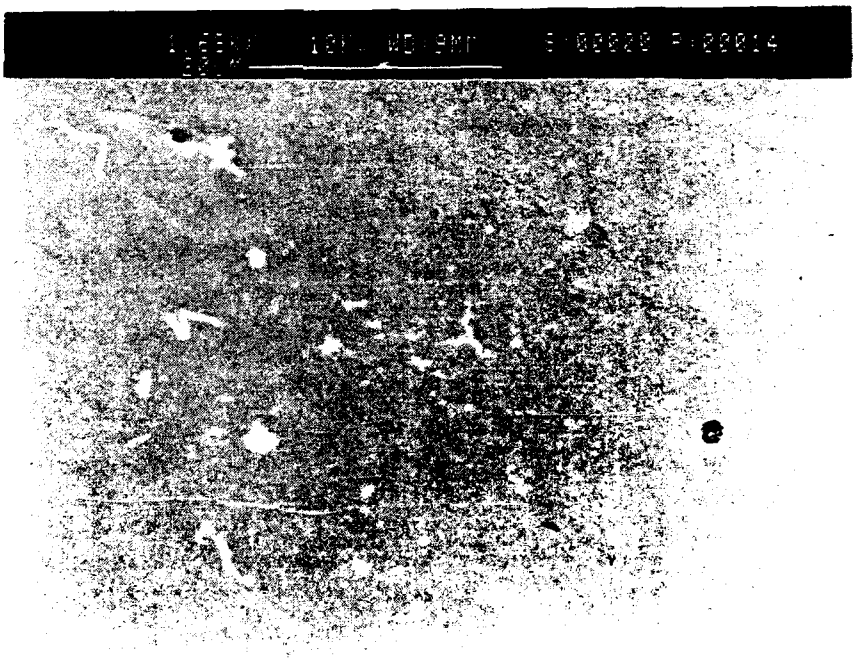

Figure 33: Scanning electron micrograph of the interior of Sample #2, representative of the area labeled as "A" in the left half sketch of the sample as depicted in Figure 32.

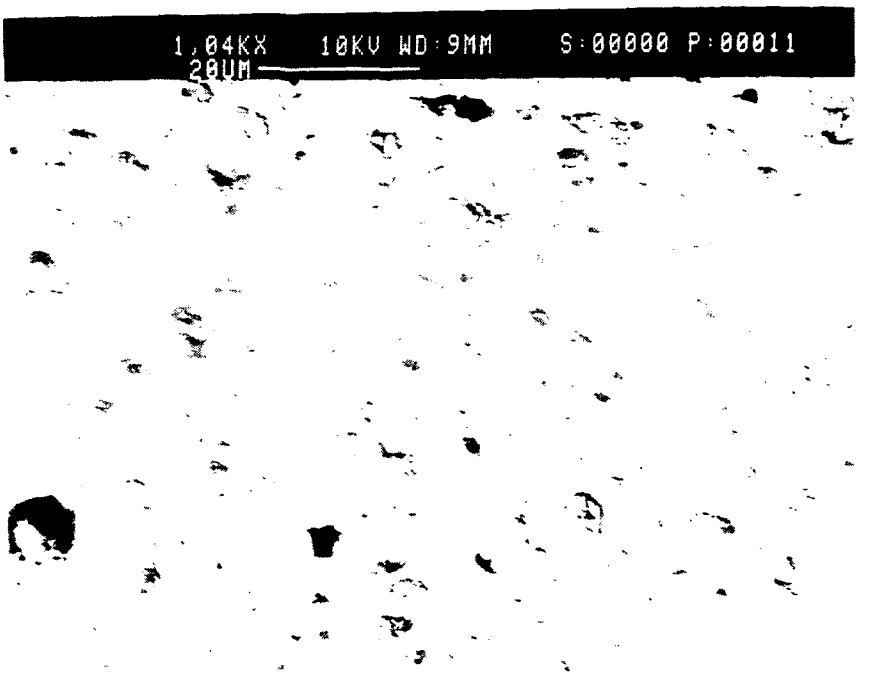

Figure 34: Scanning electron micrograph of the interior of Sample #2, representative of the area labeled as "B" in the left half sketch of the sample as depicted in Figure 32.

Figure 35: Scanning electron micrograph of the interior of Sample #2, representative of the area labeled as "C" in the left half sketch of the sample as depicted in Figure 32.

Figure 36: Scanning electron micrograph of the interior of Sample #2, representative of the area labeled as "A" in the right half sketch of the sample as depicted in Figure 32.

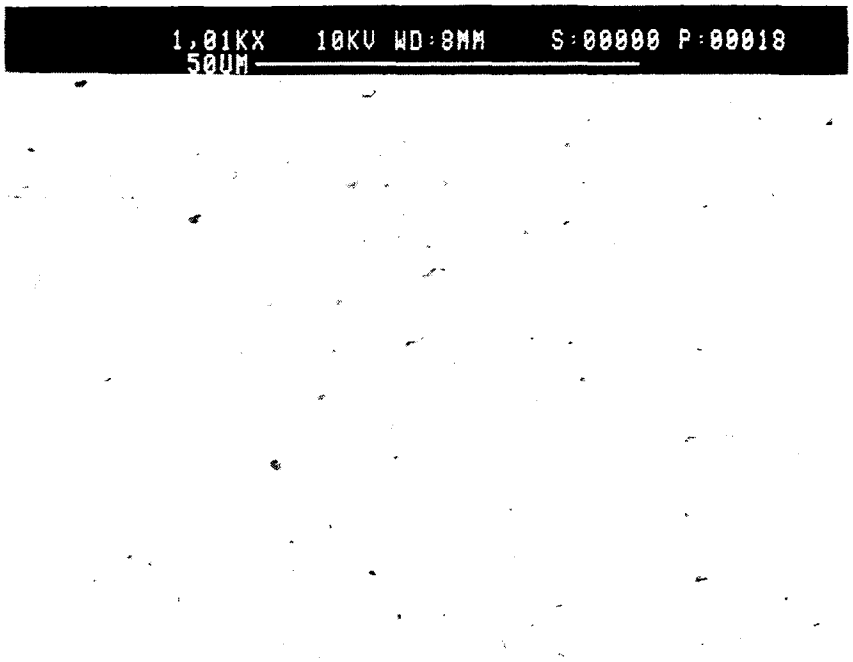

Figure 37: Scanning electron micrograph of the interior of Sample #2, representative of the area labeled as "B" in the right half sketch of the sample as depicted in Figure 32.

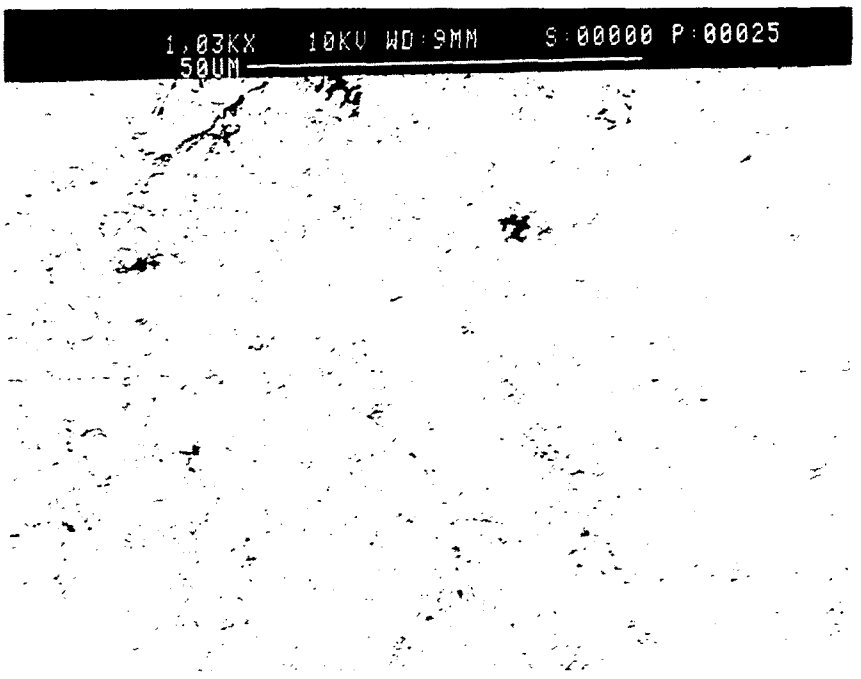

Figure 38: Scanning electron micrograph of the interior of Sample #2, representative of the area labeled as "C" in the right half sketch of the sample as depicted in Figure 32.

For the 0.02 μm powder, compressed to 50 MPa and surrounded first by alumina powder then graphite powder (Sample #3), temperatures were lower and remained in the range 1000 - 1200 Deg C (Fig. 39).

For Samples #2 and #3, the curves reached a peak in 50 seconds and then dropped approximately 400 Deg C for the next 20 seconds before climbing again. This may be due to the microwave oven having an automatic off cycle at the end of 50 seconds or an unsteady power source. Alternatively, when the pellet reached 1400 Deg C, the alumina acted as a heat sink and absorbed the heat energy as it initiated sintering. Because this phenomenon occured whether the sample actually

showed signs of sintering or not (Sample #2 and Sample #3), it cast doubt on the heat sink arguement. This temperature curve characteristic did not occur for Sample #1, so it may not be a function of the microwave operation either. More experimentation will need to be done to explain this.

The optical micrograph showed little, if any, sintering had occurred (Fig. 40). The large glassy region shown on Sample #1 (Fig. 22) also occured in lesser degree on Sample #3. An EDX of the glassy area revealed nothing even when the sample was tilted toward the beam. This glassy area may have been excessively charging to prevent proper sampling. An EDX of the area surrounding the glassy portion indicated that only pure alumina was present.

A scanning electron micrograph of the surface showed very little sintering had occured (Fig. 41). A scanning electron micrograph of the interior also showed it to remain in a nearly unsintered state (Fig. 42).

For Sample #3, temperatures remained in the range 1000 - 1200 Deg C. The alumina powder may have acted as a thermal insulator to prevent the surface of the pellet from reaching sintering temperatures. Alternatively, since the magnetron failed immediately after this sample, temperatures may not have been reached because the magnetron was already degraded. The jagged peaks and valleys may indicate magnetron output difficulties.

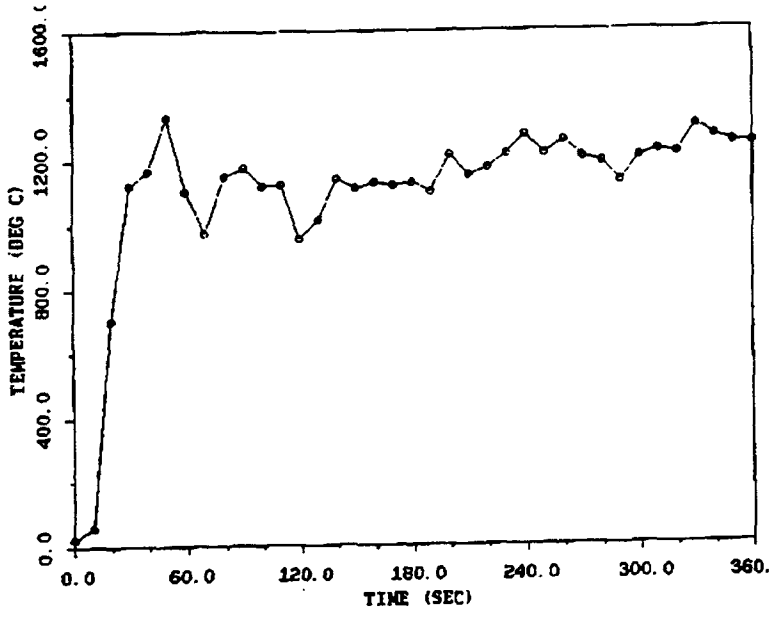

Figure 39: Temperature plot of the 0.02 μm powder, compressed to 50 MPa and surrounded first by alumina powder (0.02 μm) then graphite powder (Sample #3).

Figure 40: Optical micrograph showing unsintered surface (Sample #3).

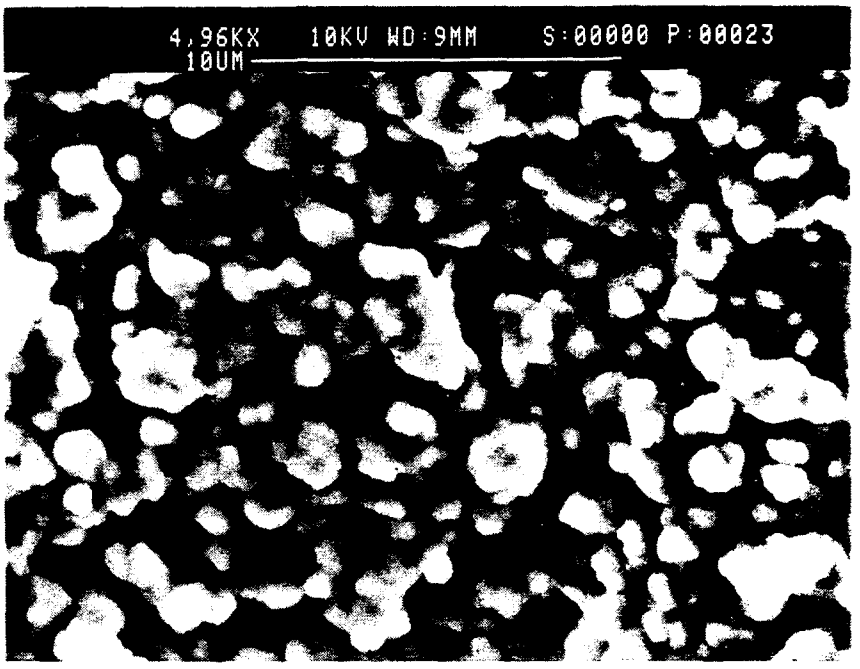

Figure 41: Scanning electron micrograph showing partial sintering (Sample #3).

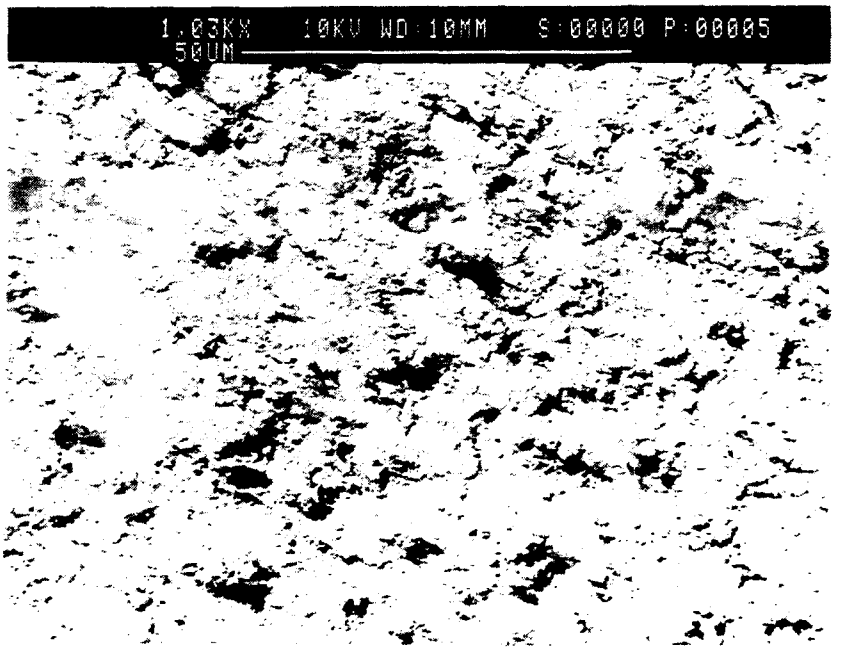

Figure 42: Scanning electron micrograph of the interior (Sample #3).

For the 0.02 μm powder, compressed to 200 MPa and surrounded by graphite powder (Sample #4), temperatures exceeded 1400 Deg C (Fig. 43). The abnormal temperature behavior that occurred within the first 50 seconds of the experimental run was due to either microwave interference with the temperature measurement system or difficulties with magnetron performance. It has been recorded in the literature [Ref. F1] that there are instances where microwave radiation interfered with thermocouple measurements at low temperatures until the sample reached the critical temperature and coupled readily with the microwave field. The magnetron used in this run was new since magnetron failure occured immediately after Sample #3 was sintered. Though this new magnetron (manufactured by Goldstar™) was a recommended and less expensive replacement for the originally installed magnetron (manufactured by Panasonic™), it survived only 120 seconds when applied towards the sintering of Sample #4. Alternatively, the thermocouple leads may have been shorted prior to the run and the problem was corrected when the thermocouple wire was moved.

An optical micrograph of the surface showed localized sintering (Fig. 44). A scanning electron micrograph of the surface showed the initial stages of sintering at the outer edges of the sample (Fig. 45) and more advanced stages of sintering near the center (Fig. 46). A scanning electron micrograph of the interior showed little sintering (Fig. 47).

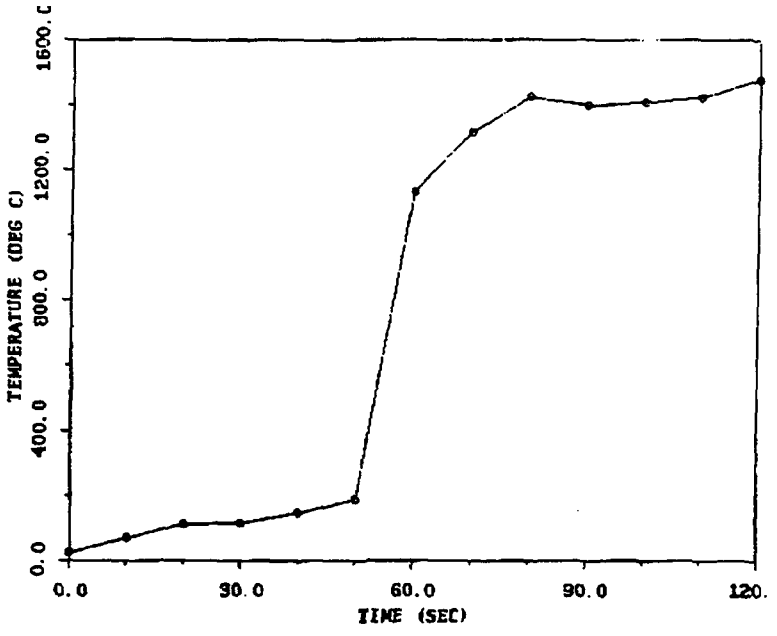

Figure 43: Temperature plot of the 0.02μm alumina powder, compressed to 200 MPa, and surrounded by graphite powder (Sample #4).

Figure 44: Optical micrograph showing localized sintering (Sample #4).

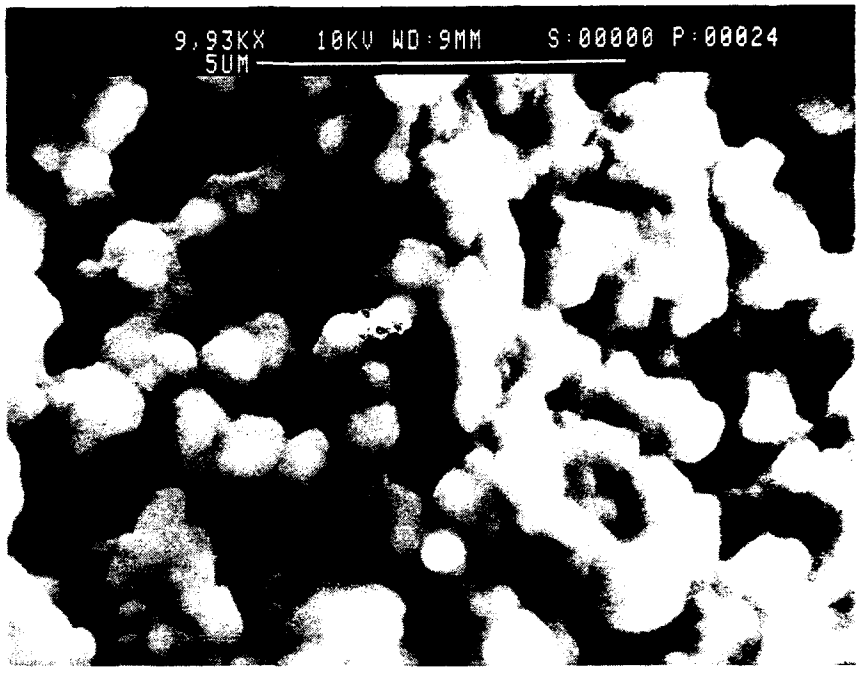

Figure 45: Scanning electron micrograph of the surface showing initial stages of sintering (Sample #4).

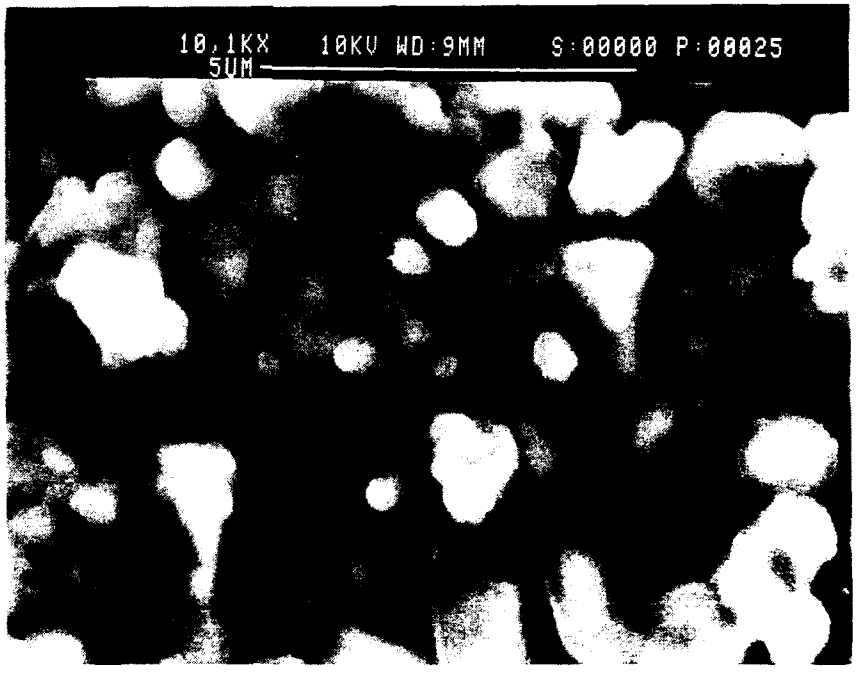

Figure 46: Scanning electron micrograph of the surface showing advanced stages of sintering (Sample #4).

Figure 47: Scanning Electron micrograph of the interior (Sample #4).

Assuming that the variations in the sample and susceptor material had less significance than the electric field strength with regard to heating rate (see Equation 11), the trends in the graphs of Sample #'s 1, 2, and 3, may describe the microwave field output as the magnetron degrades with increasing number of experimental runs. The curve of Sample #4 was an exception since the magnetron failed during the first operational attempt. Sample #'s 1, 2 and 4 indicated signs of sintering on the surface, while Sample #3 did not. Because Sample #3 was surrounded by alumina powder this may have acted as a thermal insulator preventing thermal conduction from the graphite powder to the pellet. Possibly because of this, the sample temperatures were very low, 1000 to 1200 Deg C, and the

critical temperature for sintering this sample may not have been achieved.

D. CONCLUSIONS

From the graphs it is evident that initial heating rates were very high, on the order of 50-75 Deg C/sec. The general shape of the temperature curves indicated high initial temperature rates leveling off above approximately 1400 Deg C for the sample which showed sintering. The maximum temperature obtained by the apparatus was 1575 Deg C.

Samples which were surrounded by graphite powder achieved temperatures exceeding 1400 Deg C, while the sample surrounded by alumina powder then carbon graphite powder obtained lower temperatures. It is possible that the alumina acted as a thermal insulator to prevent heat from being conducted from the graphite carbon powder to the alumina pellet. From the scanning electron micrographs, it was evident that sintering had occurred but typically in localized areas. Generally, better sintering occurred at the sample interior than at or near the surface.

The region of the sample near where the thermocouple probe tip was in contact with the sample appeared to have sintered very well. It is possible that the probe's small tip diameter concentrated the electromagnetic field at the tip. The higher field concentration corresponded to a higher power dissipation in the local area.

Only localized sintering, was observed near the region of contact with the thermocouple probe, and parts of the interior of the sample near its center. This may be attributed to the graphite powder rapidly coupling with the microwave energy, obtaining high heating rates and elevated temperature levels, but possibly, absorbing most of the radiation itself and permitting little of the microwave energy to pass into the sample.

The life of the magnetron was found to be inordinately short under the operating conditions. This may have been caused by absorption of the microwaves occuring only over a very small fraction of the oven cavity occupied by the susceptor material and the sample, allowing most of the microwaves to be reflected off the cavity walls back into the magnetron.

E. SUGGESTIONS FOR FURTHER WORK

Further work is necessary to develop this technique into one which allows routine sintering of ceramic powders.

A temperature feedback controller will be necessary to control temperature heating rates, maximum and minimum temperature limits, and temperature cooling rates.

A larger crucible to incorporate larger amounts of susceptor material is necessary to absorb more of the microwave energy field, thereby returning less reflected microwave energy back to the magnetron. This will minimize

magnetron degradation due to overheating, enhance consistent operational performance of the device and extend its useful life.

Another susceptor material like SiC should replace the graphite powder. The ideal susceptor material should couple readily with microwave energy and heat up rapidly (at least up to 1000 Deg C) and yet allow some of the microwave radiation to be transmitted through to reach the sample material itself, similar to a picket fence arrangement discussed in the literature.

An understanding of why sintering is confined to one area of the sample must be established. A series of experiments to determine if the location of the sample within the cavity influences the localized sintering behavior observed. Alternatively, the location of the temperature probe in relation to the sample could be varied to determine if a higher field concentration is developed by the probe which produces higher power dissipation in a localized area. If the concentration of the temperature field at the probe tip appears to increase sintering efficiency, small metal ball bearings may be kept in contact with the sample to allow field concentration over a larger area of the sample.

LIST OF REFERENCES

B1. Binner, J.G.P., *Advanced Ceramic Processing and Technology,* v.1, Noyes Publications, pp. 285-367, 1990.

B2. Binner, J.G.P., "Microwave Sintering of Advanced Materials," *Advanced Materials Supplement,* p. AM3, May 1992.

B3. Binner, J.G.P. and Cross, T.E. "Applications from Temperature Profile Control During Microwave Sintering," *Fabrication Science and Technology,* Institute of Ceramics, December 18-20, 1991.

B4. Binner, J.G.P.,"Applications of Microwaves in the sintering of ceramics," *The Institute of Electrical Engineers,* colloquium held on June 20, 1990.

B5. Bruce, R.W. "New Frontiers in the Use of Microwave Energy: Power and Metrology," *Materials Research Society Symposium Proceedings,* v. 124, pp. 3-15, Materials Research Society, 1988.

B6. Brook, R.J., "Fabrication Principles for the Production of Ceramics with Superior Mechanical Properties," *British Ceramic Society,* v. 32, pp. 7-14, 1982.

B7. Blake, R.D. and Meek, T.T., "Microwave processed composite materials," *Journal of Material Science Letters,* v. 5, pp. 1097 - 1098, 1986.

C1. Calister, W., *Materials Science and Engineering an Introduction,* 2d ed., p. 393, John Wiley and Sons, Inc., 1991.

C2. Chabinsky, I.J., "Applications of Microwave Energy Past, Present, and Future 'Brave New Worlds'," *Materials Research Society Symposium Proceedings,* v. 124, pp. 17-29, Materials Research Society, 1988.

F1. Fang, Y., Agrawal, D.K., Roy, D.M. and Roy R., "Microwave Sintering of Hydroxyapatite Ceramics," *Journal of Materials Research,* v. 9, no.1, p. 181, January 1994.

F2. Ford, J.D. and Pei, D.C,T., "High Temperature Chemical Processing via Microwave Absorption," *Journal of Microwave Processing,* v.2, no. 2, pp. 61-64, 1967.

G1. Telephone Conversation Between John Gerling, Gerling Labs, Modesto, CA and the Author, December, 1993.

H1. Holcombe, G.E., Meek, T.T. and Dykes, N., "Enhanced Thermal Shock Properties of Y_2O_3-2wt% ZrO_2 Heated Using 2.45 GHz Radiation," *Materials Research Society Symposium Proceedings,* v. 124, pp. 227-234, Materials Research Society, 1988.

H2. Harrison, W.B., Hanson, M.R.B. and Koepke, B.G.,"Microwave Processing and Sintering of PZT and PLZT Ceramics," *Materials Research Society Symposium Proceedings,* v. 124, pp. 279-286, Materials Research Society, 1988.

H3. Ho, W.W., "High-Temperature Dielectric Properties of Polycrystalline Ceramics," *Materials Research Society Symposium Proceedings,* v. 124, pp. 137-148, Materials Research Society, 1988.

I1. Inglesias, J. and Westphal, W.B., "Supplementary Dielectric Constants and Loss Measurements on High Temperature Materials,"Technical Report no. 203, MIT, January, 1967.

J1. Janney, M.A., Calhoun, C.L. and Kimrey, H.D., "Microwave Sintering of Solid Oxide Fuel Cell Materials: I, Zirconia-8 mol% Yittria," *Journal of American Ceramic Society,* v. 75, no. 2, pp. 341-346, 1992.

J2. Janney, M.A., Kimrey, H.D., Schmidt, M.A. and Kiggans, J.O., "Grain Growth in Microwave Annealed Alumina," *Journal of American Ceramic Society,* v. 74, no. 7, pp.1675-1681, 1991.

J3. Janney, M.A., Kimrey, H.D. and Kiggans, J.O., "Microwave Processing of Ceramics," *Materials Research Society Symposium Proceedings,* v. 269, pp. 173-185, Materials Research Society, 1992.

J4. Johnson, D.L., Tian, Y.L. and Brodwin, M.E. "Ultrafine Structure of Al_2O_3 Produced by Microwave Sintering," *Proceeding First International Conference on Ceramic Powder Processing Science,* Orlando, Florida, November 1987.

K1. Kimrey H.D., Janney M.A. and Becher P.F., "Techniques for Ceramic Sintering Using Microwave Energy," *IEEE,* p.136, 1987.

K2. Kimrey, H.D. and Janney, M.A., "Design Priciples for High-Frequency microwave Cavities," *Materials Research Society Symposium Proceedings,* v. 124, p.367, Materials Research Society, 1988.

K3. Kimrey, H.D., White, T.L. and Bigelow, T.S., "Initial Results of High-Power Microwave Sintering Experiments at ORNL," CONF-860743-1, DE 86,010041.

K4. Krage, M., "Microwave Sintering of Ferrites," *American Ceramic Society Bullitin,* v. 60, no. 11, pp. 1232-1234, 1981.

L1. Lorenson, C., "The Why's and How's of Mathematical Microwave Heating," *Microwave World,* v. 11, no. 1, Spring 1992.

M1. Q.B. Products, "Microwave Oven Replacement Parts Product Catalog II." Mack Stove Co., p. 7, 1994.

M2. Metaxes, A.C. and Binner, J.G.P., "Microwave Processing of Ceramics," *Advanced Ceramic Processing and Technology,* v. 1, pp. 285-367, Noyes Publications, 1990.

M3. Maguire, E.A., Reary, D.W., "Microwave Absorbing Ferrite-Dielectric Composites," *Journal of American Ceramic Society,* v. 59, no. 9, pp. 434-437, 1976.

M4. Meek, T.T., Dykes, N. and Holcombe, C.E., "Microwave Sintering of Some Oxides Using Sintering Aids," *Journal of Materials Science Letters,* v.6, pp. 1060-1062, 1987.

M5. Meek, T.T., Blake, R.D. and Petrovic J.J., "Microwave Sintering of Al_2O_3-SiC Whisker Composites," *Ceramic Engineering and Science Proceedings,* v. 8, no. 7-8, pp. 861-871, 1987.

M6. Metaxes, A.C., "A Unified Approach to the Teaching of Electromagnetic Heating of Industrial Materials," *International Journal of Electrical Engineering Education,* v. 22, pp. 101-118, Manchester U.P., 1985.

M7. Metaxes, A.C. and Meredith, R., *Industrial Microwave Heating,* Peter Peregrinus, 1983.

P1. Patil, D., Mustang, B. and Garard, R.,"Microwave Reaction Sintering of Oxide Ceramics," *Journal of Microwave Power and Electromagnetic Energy,* v. 27, no. 1, pp. 49-53, International Microwave Power Institute, 1992.

P2. Puchner, H., *Heating with Microwaves,* p. 2, Springer-Verlag, New York, Inc., 1966.

R1. Richerson, D., *Modern Ceramic Engineeering Properties, Processing, and Use in Design,* pp. 149-260, Marcel Dekkar, Inc., 1982.

R2. Richerson, D., *Modern Ceramic Engineering Properties, Processing, and Use in Design,* 2d ed., pp.373-597, John Wiley and Sons, Inc., 1992.

S1. Samuels, J. and Brandon, J.R., "Effect of Composition on the Enhanced Microwave Sintering of Alumina-Based Ceramic Composites," *Journal of Materials Science,* v. 27, pp. 3259-3265, Chapman and Hall, 1992.

S2. Sutton, W.H., "Microwave Processing of Ceramics - an Overview," *Journal of Materials Science,* v. 124, pp. 3-21, Chapman and Hall, 1992.

S3. Stuchly, S.S. and Hamid, M.A.K., "Physical Parameters in Microwave Heating Processes," *Journal of Microwave Power,* v.7, no. 2, pp. 117-137, 1972.

S4. Sutton, W.H., "Microwave Processing of Ceramic Material," *Ceramic Bulletin,* v. 68, no. 2, 1989.

S5. Sutton, W.H., "Microwave Firing of High Alumina Castables," *Materials Research Society Symposium Proceedings,* v. 124, pp. 287-295, Materials Research Society, 1988.

S6. Sutton, W.H. and Johnson, W.E., U.S. Patent No. 4,140,887 (20 Feb 1979).

T1. Tinga, W.R., "Design Principles for Microwave Heating and Sintering," *Materials Research Society Symposium Proceedings,* v. 60, pp. 105-116, Materials Research Society, 1988.

T2. Tinga, W.R., "Fundamentals of Microwave-Material Interactions and Sintering," *Materials Research Society Symposium Proceedings,* v. 124, pp. 33-34, Materials Research Society, 1988.

T3. Tao, J.L., "A New Type of Microwave Sintering Apparatus Using Microwave Heating," *Chinese Science Bulleting,* v. 36, no.11, pp. 900-902, Shanghai Institute of Ceramics, Chinese Academy of Sciences, June 1991.

T4. Tinga, W.R. and Voss, A.G., *Microwave Power Engineering,* academic Press, New York, 1968.

V1. Von Hippel, A.R., *Dielectric Materials and Applications,* John Wiley and Sons, Inc., New York, 1954.

W1. Wroe, F.C.R. and Samuels J., "Microwave Sintering of Advanced Ceramics," *Fabrication Science and Technology,* Institute of Ceramics, December 18-20, 1991.

W2. Wilson, J. and Kunz, S.M., "Microwave Sintering of Partially Stabilized Zirconia," *Journal of American Ceramic Society,* v.71, no. 1, pp. C40-41, 1988.

W3. Westphal, W.B. and Sils, A. "Dielectric Constant and Loss Data," AFML-TR-74-250, parts I-IV, Apr 1972 - Dec 1980.

Y1. Yonnone, M., "Microwave equipment considerations for High Temperature Studies in Ceramics," *Materials Research Society Symposium Proceedings,* v. 124, pp. 373-377, Materials Research Society, 1988.

INITIAL DISTRIBUTION LIST

		No. Copies
1.	Defense Technical Information Center Cameron Station Alexandria VA 22304-6145	2
2.	Library, Code 052 Naval Postgraduate School Monterey CA 93943-5002	2
3.	Naval Engineering Curricular Office, Code 34 Naval Postgraduate School Monterey, CA 93943-5000	1
4.	Department Chairman, Code ME/Kk Department of Mechanical Engineering Naval Postgraduate School Monterey, CA 93943-5000	1
5.	Dr. Alan G. Fox, Code ME/Fx Department of Mechanical Engineering Naval Postgraduate School Monterey, CA 93943-5000	2
6.	Professor I. Dutta, Code ME/Du Department of Mechanical Engineering Naval Postgraduate School Monterey, CA 93943-5000	2
7.	LT Edgar M. Alhambra 1419 Kenneth Street Seaside, CA 93955	4